A study of heavy flavoured meson fragmentation functions in e^+e^- annihilation

Matteo Cacciari

LPTHE, Université Pierre et Marie Curie (Paris 6)
France
E-mail: `cacciari@lpthe.jussieu.fr`

Paolo Nason

INFN, Sezione di Milano
Piazza della Scienza 3, 20126 Milan, Italy
E-mail: `Paolo.Nason@mib.infn.it`

Carlo Oleari

Università di Milano-Bicocca
Piazza della Scienza 3, 20126 Milan, Italy
E-mail: `carlo.oleari@mib.infn.it`

ABSTRACT: We compare QCD theoretical predictions for heavy flavoured mesons fragmentation spectra in e^+e^- annihilation with data from CLEO, BELLE and LEP. We include several effects in our calculation: next-to-leading order initial conditions, evolution and coefficient functions. Soft-gluon effects are resummed at next-to-leading-log accuracy. A matching condition for the crossing of the bottom threshold in evolution is also implemented at next-to-leading order accuracy. Important initial-state electromagnetic radiation effects in the CLEO and BELLE data are accounted for. We find that, with reasonably simple choices of a non-perturbative correction to the fixed-order initial condition for the evolution, the data from CLEO and BELLE can be fitted with remarkable accuracy. The fitted fragmentation function, when evolved to LEP energies, does not however represent fairly the D^* fragmentation spectrum measured by ALEPH. Large non-perturbative corrections to the coefficient functions of the meson spectrum are needed in order to reconcile CLEO/BELLE and ALEPH results.

Non-perturbative parameters extracted from the fits to e^+e^- fragmentation data for D/D^* and B mesons are tabulated. They can be employed in the theoretical predictions for the production of charmed and bottomed mesons in hadron-hadron, photon-hadron and photon-photon collisions.

KEYWORDS: QCD, e+-e- Experiments, NLO Computations, Heavy Quarks Physics.

Contents

1. Introduction

The study of the fragmentation functions of heavy flavoured hadrons is of considerable interest in several aspects of QCD and collider physics. On one hand, at transverse momenta much larger than the mass of the heavy flavour, the heavy-flavour fragmentation functions behave similarly to the light-hadron ones, and obey an Altarelli-Parisi evolution equation. Unlike the case of light hadrons, however, heavy-flavour fragmentation is very hard, and thus probes a region of the evolution equation in the large x regime. Furthermore, it is dominated by the non-singlet component, at least at moderate energies, so that its study is much simpler.

Due to the large value of the heavy-quark mass m, the heavy-quark fragmentation function has a well defined perturbative expansion in QCD. In typical production phenomena, like for example heavy-flavour production in e^+e^- annihilation, the coefficients of the perturbative result contain large logarithms of the ratio Q/m, where Q is the annihilation energy. These logarithms can be organized using the standard Altarelli-Parisi evolution formalism, so that the perturbative result is expressed as a perturbative initial condition for the fragmentation function [1], written as expansion in powers of $\alpha_{\rm S}(m)$, evolved at the high scale Q, using standard evolution. Sudakov logarithms that affect the $x \to 1$ region can be resummed to all orders too [2]. In this framework, the description of non-perturbative effects that affect the initial condition of the fragmentation function are parametrized by simple phenomenological forms. These parameterizations can then be employed to provide theoretical predictions for charmed and bottomed hadron production in hadron-hadron, photon-hadron and photon-photon collisions.

Recently, new, high quality data on charmed meson production have come from CLEO [3] and BELLE [4]. One thus has the opportunity to perform a more accurate fit to the non-perturbative initial conditions, and furthermore one can test the evolution of the fragmentation function from centre-of-mass energies of 10.6 to 91.2 GeV, using charm data from LEP experiments. In the present work we will carry out this program. We develop a procedure that overcomes various difficulties in the large-x region of the fragmentation function. We are thus able to fit the measured fragmentation functions using next-to-leading logarithmic (NLL) evolution, next-to-leading order (NLO) initial conditions, NLO coefficient functions, NLL Sudakov resummation (both for the initial conditions and for the coefficient functions) and a phenomenological non-perturbative component. With a suitable choice of this non-perturbative component we can obtain very good fits to CLEO and BELLE data for D^* and D fragmentation, over the whole x range. All the moments of the fragmentation functions are therefore well reproduced. This represents an improvement over previous investigations where, while obtaining good fits to some low moments (a necessary and sufficient condition for predicting heavy-meson production in hadronic collisions) the fit in x-space was not completely satisfactory. The same procedure is also applied to B meson spectra measured in Z^0 decays. The relevant data from the ALEPH [5] OPAL [6], SLD [7] and DELPHI [8, 9] collaborations are equally well described.

We evolve the D^* fragmentation function fitted to CLEO and BELLE data up to LEP energies, taking into account the opening of the bottom threshold [10]. We find a discrepancy between the QCD prediction and the ALEPH data [11], that can be parametrized as a power correction of the form $C(N-1)/E$, with C of the order of few hundreds MeV, or of the form $C(N-1)/E^2$, with $C \approx 5$ GeV^2, where $E = \sqrt{q^2}$ is the total centre-of-mass energy and N is the moment in Mellin space. Unfortunately, there is no way, at the moment, to discriminate between the two possibilities. Theoretical arguments based upon renormalons disfavour the presence of $1/E$ corrections in the evolution of fragmentation functions. On the other hand, these arguments require validation.

In section 2 we describe the theoretical ingredients that enter our calculation, collecting and summarizing previously available results: the perturbative initial condition, the evolution, the Sudakov effects and the bottom threshold. The novel treatment of the large-

N/large-x region is also detailed here. In section 3 we describe our treatment of electromagnetic initial-state radiation. The implementation of the non-perturbative component of the fragmentation function is discussed in section 4. In section 5 we perform fits to the CLEO and BELLE data. In Section 6 we compare the evolved CLEO/BELLE D^* fit to the ALEPH data, and discuss in detail the related problems. Fits for B meson production are presented in section 7. In section 8, we perform fits to data under a different perspective, using Mellin moments rather than the x-space distributions, and employing a simpler, one-parameter non-perturbative function, that can be related to Λ/m power corrections. The implications of the new BELLE and CLEO data for heavy-flavour hadroproduction are also discussed in this section. Finally, in section 9, we give our conclusions.

2. Theoretical framework

We consider the inclusive production of a heavy quark Q of mass m

$$e^+e^- \to Z/\gamma\,(q) \to Q\,(p) + X\,, \tag{2.1}$$

where q and p are the four-momenta of the intermediate boson and of the final quark. We define x as the scaled energy of the final heavy quark,

$$x \equiv \frac{2\,p \cdot q}{q^2}\,. \tag{2.2}$$

In our framework, we neglect corrections suppressed by powers of the heavy-quark (meson) mass, and so the above definition may be replaced with the usual experimental definition of scaled momentum (i.e. the heavy flavoured meson momentum over its maximum value). The inclusive cross section for the production of the heavy quark Q can be written as a perturbative expansion in $\alpha_{\rm s}$

$$\frac{d\sigma_Q}{dx}(x, q^2, m^2) = \sum_{n=0}^{\infty} \bar\alpha_s^n(\mu^2)\,\sigma_Q^{(n)}(x, q^2, m^2, \mu^2)\,, \tag{2.3}$$

where $E = \sqrt{q^2}$ is the total centre-of-mass energy, μ is the renormalization scale, and

$$\bar\alpha_s(\mu^2) \equiv \frac{\alpha_{\rm s}(\mu^2)}{2\pi}\,. \tag{2.4}$$

The cross section (2.3), normalized to the total cross section, is sometimes referred to as the heavy-quark fragmentation function in e^+e^- annihilation.

In order not to spoil the convergence of eq. (2.3), the coefficients $\sigma_Q^{(n)}$ should be small enough to justify a perturbative expansion in terms of $\alpha_{\rm s}$. There are, however, at least two interesting regions of the parameter phase space where such convergence is undermined:

1. If $q^2 \gg m^2$, large logarithms of the form $\log(q^2/m^2)$ appear in the differential cross section (2.3) to all orders in the perturbative expansion. These logarithms have collinear origin, and the mass m acts as a regulator.

2. In the region of the phase space of multiple soft-gluon emission, i.e. $x \rightarrow 1$, the differential cross section contains enhanced terms proportional to $\log^n(1-x)/(1-x)$.

In the following two sections, we collect the relevant formulae for the resummation of these large contributions at the next-to-leading log level.

2.1 Collinear logarithms

In the limit where power terms of the ratio m^2/q^2 can be neglected, the differential cross section satisfies the factorization theorem

$$\frac{d\sigma_{P,Q}}{dx}(x,q^2,m^2) = \sum_i \int_x^1 \frac{dz}{z} \, C_{P,i}\left(z,q^2,\mu^2\right) \, D_i\left(\frac{x}{z},\mu^2,m^2\right), \qquad (2.5)$$

where the subscript P stands for either T for transverse, L for longitudinal, A for asymmetric or nothing for the total (i.e. L+T) cross section.[1] In the following, we shall always drop the polarization subscript, since we shall always refer to total cross sections.

The C_i coefficients are the $\overline{\text{MS}}$-subtracted partonic cross sections for producing the massless parton i, and D_i are the $\overline{\text{MS}}$ fragmentation functions for parton i to evolve into the heavy quark Q. The factorization scale μ^2 must be taken of order q^2 in order to avoid the appearance of large logarithms of q^2/μ^2 in the partonic cross section. The explicit expressions for the partonic cross sections and for the fragmentation functions at NLO can be found in refs. [1, 12].

The $\overline{\text{MS}}$ fragmentation functions D_i obey the Altarelli-Parisi evolution equations[2]

$$\frac{dD_i}{d\log\mu^2}(x,\mu^2,m^2) = \sum_j \int_x^1 \frac{dz}{z} \, P_{ji}\left(\frac{x}{z},\bar\alpha_s(\mu^2)\right) \, D_j(z,\mu^2,m^2). \qquad (2.6)$$

The Altarelli-Parisi splitting functions P_{ji} have the perturbative expansion

$$P_{ji}\left(x,\bar\alpha_s(\mu^2)\right) = \bar\alpha_s(\mu^2)P_{ji}^{(0)}(x) + \bar\alpha_s^2(\mu^2)P_{ji}^{(1)}(x) + \mathcal{O}(\bar\alpha_s^3), \qquad (2.7)$$

where the $P_{ji}^{(0)}$ are[3] [13]

$$P_{qq}^{(0)}(z) = C_F\left[\frac{1+z^2}{(1-z)_+} + \frac{3}{2}\delta(1-z)\right],$$

$$P_{gg}^{(0)}(z) = 2C_A\left[\frac{z}{(1-z)_+} + \frac{1-z}{z} + z(1-z) + \left(\frac{11}{12} - \frac{n_{\mathrm{f}}T_F}{3C_A}\right)\delta(1-z)\right],$$

$$P_{gq}^{(0)}(z) = C_F\frac{1+(1-z)^2}{z},$$

$$P_{qg}^{(0)}(z) = T_F\left[z^2 + (1-z)^2\right], \qquad (2.8)$$

---

[1]We follow closely the notation of ref. [12].

[2]Notice that the splitting functions are transposed with respect to the structure function evolution equations.

[3]The + distribution is defined as

$$\int_0^1 dz \, h(z) \, [\,g(z)\,]_+ \equiv \int_0^1 dz \, [h(z) - h(1)] \, g(z).$$

n_{f} is the number of active flavours and

$$C_A = 3, \quad C_F = \frac{4}{3}, \quad T_F = \frac{1}{2}. \tag{2.9}$$

The NLO splitting functions $P_{ji}^{(1)}$ (needed to achieve NLL accuracy) have been computed in refs. [14–18]. They are too lengthy to be replicated here.

The initial conditions for the $\overline{\mathrm{MS}}$ fragmentation functions were first obtained at the NLO level in ref. [1]. They are given by

$$D_Q(x, \mu_0^2, m^2) = \delta(1-x) + \bar{\alpha}_s(\mu_0^2) \, d_Q^{(1)}(x, \mu_0^2, m^2) + \mathcal{O}(\bar{\alpha}_s^2), \tag{2.10}$$

$$D_g(x, \mu_0^2, m^2) = \bar{\alpha}_s(\mu_0^2) \, d_g^{(1)}(x, \mu_0^2, m^2) + \mathcal{O}(\bar{\alpha}_s^2), \tag{2.11}$$

(all the other components, of order $\bar{\alpha}_s^2$, are beyond the accuracy of the present calculation and have been computed in refs. [19, 20]), where

$$d_Q^{(1)}(x, \mu_0^2, m^2) = C_F \left[\frac{1+x^2}{1-x} \left(\log \frac{\mu_0^2}{m^2} - 2\log(1-x) - 1 \right) \right]_+, \tag{2.12}$$

$$d_g^{(1)}(x, \mu_0^2, m^2) = T_F \left[x^2 + (1-x)^2 \right] \log \frac{\mu_0^2}{m^2}. \tag{2.13}$$

In order to compute the NLL resummed fragmentation function, one takes the initial conditions at a scale $\mu_0 \simeq m$, evolves them up to $\mu \simeq E$ (these choices for μ_0 and μ prevent the appearance of large logarithms that would spoil the NLL accuracy), and then applies eq. (2.5), using the NLO expression for the partonic cross sections C_i given in eqs. (2.15) of ref. [12][4]

$$C_q(z, q^2, \mu^2) = \left[\delta(1-z) + \bar{\alpha}_s a_q^{(1)} \left(z, \frac{\mu^2}{q^2} \right) \right] \sigma_{0,q}(q^2), \tag{2.14}$$

$$C_g(z, q^2, \mu^2) = \bar{\alpha}_s a_g^{(1)} \left(z, \frac{\mu^2}{q^2} \right) \sigma_{0,g}(q^2), \tag{2.15}$$

where, to make contact with the notations of refs. [1, 12], we have defined

$$a_{q/g}^{(1)} \left(z, \frac{\mu^2}{q^2} \right) \equiv C_F c_{q/g} \left(z, \frac{\mu^2}{q^2} \right). \tag{2.16}$$

The procedure outlined above guarantees that all leading and next-to-leading logarithmic terms of quasi-collinear origin (terms of the form $(\bar{\alpha}_s \log(q^2/m^2))^n$ and $\bar{\alpha}_s(\bar{\alpha}_s \log(q^2/m^2))^n$ respectively) are correctly resummed in the final cross section.

---

[4]In this work, we complement the Born electroweak cross section with a threshold factor for the heavy quarks (and antiquarks)

$$\sigma_{0,q}(q^2) \to \sigma_{0,q}(q^2) \left(1 + \frac{2m_q^2}{q^2} \right) \sqrt{1 - \frac{4m_q^2}{q^2}},$$

for $q = c, b$. Its numerical impact is, however, negligible at the energies considered here.

When dealing with the type of convolution appearing in eqs. (2.5) and (2.6), it is customary to introduce the Mellin transform

$$f(N) \equiv \int_0^1 dx\, x^{N-1} f(x)\,.\tag{2.17}$$

We adopt the convention that, when N appears instead of x as the argument of a function, we are actually referring to the Mellin transform of the function. The Mellin transform of the factorization formula (2.5) is given by

$$\sigma_Q(N, q^2, m^2) = \sum_i C_i(N, q^2, \mu^2)\, D_i(N, \mu^2, m^2)\,,\tag{2.18}$$

where

$$\sigma_Q(N, q^2, m^2) \equiv \int_0^1 dx\, x^{N-1} \frac{d\sigma}{dx}(x, q^2, m^2)\,,\tag{2.19}$$

and the Mellin transform of the Altarelli-Parisi evolution equation (2.6) at NLO is

$$\frac{dD_i(N, \mu^2, m^2)}{d\log\mu^2} = \sum_j \bar\alpha_s(\mu^2)\left[P_{ji}^{(0)}(N) + \bar\alpha_s(\mu^2)P_{ji}^{(1)}(N)\right] D_j(N, \mu^2, m^2)\,.\tag{2.20}$$

2.2 Soft logarithms

Both $a_q^{(1)}$ and $d_Q^{(1)}$ contain terms associated to the emission of a soft (and collinear) gluon, These terms give rise to a large-N growth of the corresponding Mellin transforms

$$a_q^{(1)}(N, q^2, \mu^2) = C_{\rm F}\left[\ln^2 N + \left(\frac{3}{2} + 2\gamma_E - 2\ln\frac{q^2}{\mu^2}\right)\ln N + \alpha_q + \mathcal{O}\left(1/N\right)\right]\,,\tag{2.21}$$

$$d_Q^{(1)}(N, \mu_0^2, m^2) = C_{\rm F}\left[-2\ln^2 N + 2\left(\ln\frac{m^2}{\mu_0^2} - 2\gamma_E + 1\right)\ln N + \delta_Q + \mathcal{O}\left(1/N\right)\right]\,,\tag{2.22}$$

where $\gamma_E = 0.5772\ldots$ is the Euler constant and

$$\alpha_q = \frac{5}{6}\pi^2 - \frac{9}{2} + \gamma_E^2 + \frac{3}{2}\gamma_E + \left(\frac{3}{2} - 2\gamma_E\right)\log\frac{q^2}{\mu^2}\,,\tag{2.23}$$

$$\delta_Q = 2 - \frac{\pi^2}{3} + 2\gamma_E - 2\gamma_E^2 - \left(\frac{3}{2} - 2\gamma_E\right)\ln\frac{m^2}{\mu_0^2}\,.\tag{2.24}$$

In ref. [2], the all-order resummation of the large $(\ln N)$ contributions has been performed to next-to-leading log accuracy, that is, all logarithms of the form $\alpha_{\rm S}^n \ln^{n+1} N$ (leading logarithms) and $\alpha_{\rm S}^n \ln^n N$ (next-to-leading logarithms) have been correctly resummed. In the following we summarize the results of ref. [2].

The Sudakov resummation factor for the e^+e^- coefficient function can be written as

$$\Delta_q^S(N, q^2, \mu^2) = \exp\left[\ln N\, g^{(1)}(\lambda) + g^{(2)}(\lambda)\right]\,,\tag{2.25}$$

where

$$g^{(1)}(\lambda) = \frac{A^{(1)}}{\pi b_0 \lambda}\left[\lambda + (1-\lambda)\ln(1-\lambda)\right]\,,\tag{2.26}$$

$$g^{(2)}(\lambda) = \frac{A^{(1)}b_1}{2\pi b_0^3} \left[2\lambda + 2\ln(1-\lambda) + \ln^2(1-\lambda) \right] \tag{2.27}$$

$$+ \frac{\left(B^{(1)} - 2A^{(1)}\gamma_E \right)}{2\pi b_0} \ln(1-\lambda)$$

$$- \frac{1}{\pi b_0} \left[\lambda + \ln(1-\lambda) \right] \left(\frac{A^{(2)}}{\pi b_0} - A^{(1)} \ln \frac{q^2}{\mu^2} \right) - \frac{A^{(1)}}{\pi b_0} \lambda \ln \frac{q^2}{\mu^2} \,,$$

and where

$$b_0 = \frac{11C_A - 4T_F n_{\rm f}}{12\pi} \,, \qquad b_1 = \frac{17C_A^2 - 10C_A T_F n_{\rm f} - 6C_F T_F n_{\rm f}}{24\pi^2} \tag{2.28}$$

are the first two coefficients of the QCD β-function, and

$$A^{(1)} = C_{\rm F} \,, \quad A^{(2)} = \frac{1}{2} C_{\rm F} \, K = \frac{1}{2} C_{\rm F} \left[C_A \left(\frac{67}{18} - \frac{\pi^2}{6} \right) - \frac{5}{9} n_{\rm f} \right] \,, \tag{2.29}$$

$$B^{(1)} = -\frac{3}{2} C_{\rm F} \,. \tag{2.30}$$

The variable λ is defined by

$$\lambda \equiv b_0 \, \alpha_{\rm s}(\mu^2) \ln N \,. \tag{2.31}$$

The number of quark flavours in b_0 and b_1 is set to the number of active flavours at the scale μ, i.e. typically four for charm production below or near the bottom threshold, and five for charm or bottom production above the bottom threshold.

The presence in the resummed expressions of $\log(1-\lambda)$ gives rise to a cut singularity starting at the branch point

$$N_q^L = \exp \left(\frac{1}{b_0 \alpha_{\rm s}(\mu^2)} \right) \simeq \frac{\mu^2}{\Lambda_{\rm QCD}^2} \,. \tag{2.32}$$

This singularity is related to the divergent behaviour of the running coupling $\alpha_{\rm s}(\mu^2)$ near the Landau pole at $\mu \simeq \Lambda_{\rm QCD}$, and signals the onset of non-perturbative phenomena at very large values of N or, equivalently, when x is very close to its threshold value 1. This translates into an unphysical behaviour of the resummed perturbative result in this region. In Section 2.3 we describe how we have dealt with this issue.

Similarly to what has been done for the quark coefficient function, in ref. [2] the Sudakov-resummed expression for the initial condition of the fragmentation function has also been derived, yielding a result similar to eq. (2.25). To NLL accuracy we have

$$\Delta_{\rm ini}^S(N, \mu_0^2, m^2) = \exp \left[\ln N \, g_{\rm ini}^{(1)}(\lambda_0) + g_{\rm ini}^{(2)}(\lambda_0) \right] \,, \tag{2.33}$$

with

$$g_{\rm ini}^{(1)}(\lambda_0) = -\frac{A^{(1)}}{2\pi b_0 \lambda_0} \left[2\lambda_0 + (1 - 2\lambda_0) \ln(1 - 2\lambda_0) \right] \,, \tag{2.34}$$

$$g_{\rm ini}^{(2)}(\lambda_0) = \frac{A^{(1)}}{2\pi b_0} \left(\ln \frac{\mu_0^2}{m^2} + 2\gamma_E \right) \ln(1 - 2\lambda_0)$$

$$-\frac{A^{(1)}b_1}{4\pi b_0^3}\left[4\lambda_0 + 2\ln(1-2\lambda_0) + \ln^2(1-2\lambda_0)\right]$$

$$+\frac{1}{2\pi b_0}\left[2\lambda_0 + \ln(1-2\lambda_0)\right]\left(\frac{A^{(2)}}{\pi b_0}\right) + \frac{H^{(1)}}{2\pi b_0}\ln(1-2\lambda_0)\,, \qquad (2.35)$$

and

$$H^{(1)} = -C_{\rm F}\,, \qquad \lambda_0 \equiv b_0\,\alpha_{\rm S}(\mu_0^2)\ln N\,. \qquad (2.36)$$

The number of quark flavours in b_0 and b_1 for the Sudakov resummation factor of the initial condition is set to the number of light flavours at the scale $\mu_0 \simeq m$, i.e. three for charm and four for bottom. Note that, for ease of notation, both in eq. (2.25) and (2.33) the renormalization and the factorization scales have been taken equal. The full expressions for the Sudakov factors can be found in [2].

Analogously to eq. (2.25), the Sudakov-resummed part $\Delta_{\rm ini}^S$ of the heavy-quark initial condition also has cut singularities in the complex variable N. In the heavy-quark case the singularities start at the branch-point

$$N_{\rm ini}^L = \exp\left(\frac{1}{2\,b_0\alpha_{\rm S}(\mu_0^2)}\right) \simeq \frac{\mu_0}{\Lambda_{\rm QCD}}\,, \qquad (2.37)$$

i.e. at $\lambda_0 = 1/2$ in eqs. (2.34) and (2.35). Again, we defer to Section 2.3 the discussion of this problem.

For later convenience, we introduce here the expansions up to order $\alpha_{\rm S}$ of Δ_q^S and $\Delta_{\rm ini}^S$, defined in eqs. (2.25) and (2.33)

$$\Delta_q^S(N,q^2,\mu^2) = 1 + \bar\alpha_s(\mu^2)\left[\Delta_q^S(N,q^2,\mu^2)\right]_{\alpha_{\rm S}} + \mathcal{O}\left(\alpha_{\rm S}^2\right)\,, \qquad (2.38)$$

$$\Delta_{\rm ini}^S(N,\mu_0^2,m^2) = 1 + \bar\alpha_s(\mu_0^2)\left[\Delta_{\rm ini}^S(N,\mu_0^2,m^2)\right]_{\alpha_{\rm S}} + \mathcal{O}\left(\alpha_{\rm S}^2\right)\,, \qquad (2.39)$$

where

$$\left[\Delta_q^S(N,q^2,\mu^2)\right]_{\alpha_{\rm S}} = C_{\rm F}\left[\ln^2 N + \left(\frac{3}{2} + 2\gamma_E - 2\ln\frac{q^2}{\mu^2}\right)\ln N\right]\,, \qquad (2.40)$$

$$\left[\Delta_{\rm ini}^S(N,\mu_0^2,m^2)\right]_{\alpha_{\rm S}} = C_{\rm F}\left[-2\ln^2 N + 2\left(\ln\frac{m^2}{\mu_0^2} - 2\gamma_E + 1\right)\ln N\right]\,. \qquad (2.41)$$

Note that they differ from the exact coefficient function of eq. (2.21) and from the initial condition for the fragmentation function of eq. (2.22) only by terms finite in the large-N limit.

In order to merge the NLL-resummed and the NLO expressions without double-counting $\mathcal{O}(\alpha_{\rm S})$ logarithmic terms, we define the Sudakov-resummed expressions for the coefficient function and initial condition in the so-called 'log-R matching scheme' as

$$C_q^{\rm res}(N,q^2,\mu^2) = \Delta_q^S(N,q^2,\mu^2)$$
$$\times \exp\left\{\bar\alpha_s(\mu^2)\left[a_q^{(1)}(N,q^2,\mu^2) - \left[\Delta_q^S(N,q^2,\mu^2)\right]_{\alpha_{\rm S}}\right]\right\}\sigma_{0,q}(q^2)\,, \qquad (2.42)$$

$$D_Q^{\rm res}(N,\mu_0^2,m^2) = \Delta_{\rm ini}^S(N,\mu_0^2,m^2)$$
$$\times \exp\left\{\bar\alpha_s(\mu_0^2)\left[d_Q^{(1)}(N,\mu_0^2,m^2) - \left[\Delta_{\rm ini}^S(N,\mu_0^2,m^2)\right]_{\alpha_{\rm S}}\right]\right\}\,. \qquad (2.43)$$

This matching prescription differs from the one employed in ref. [2] (see eqs. (36) and (76) there). However, since the exponents in the exponentials in eqs. (2.42) and (2.43) are small (i.e. do not contain large logarithms and are of order $\alpha_{\rm s}$), the exponentials can also be expanded without loss or gain of accuracy, giving rise to different - but equivalent - matching prescriptions, among which that of ref. [2].

2.3 The large-N region

We have previously remarked how the soft-gluon resummation factors Δ_q^S and $\Delta_{\rm ini}^S$ contain singularities at large N which signal the eventual failure of perturbation theory and hence the onset of non-perturbative phenomena. The matching of perturbative results with non-perturbative physics is a delicate problem, which rests, first of all, on a proper definition of the perturbative series.

One way to address this problem is to work in the framework of infra-red renormalons. In ref. [21], the perturbative series is first improved by addition of all subleading logarithms $\alpha_{\rm s}^n \ln^k N$, with $k \leq n+1$, in the so-called large-β_0 approximation. The asymptotically divergent series is subsequently regulated either by truncation at the smallest term or with a Cauchy principal-value prescription of its Borel antitransform. This also implicitly defines non-perturbative terms which can be cast in the form of power corrections, hence allowing to relate charm and bottom hadronization. This procedure makes maximal use of the insight that can be gleaned from perturbative QCD. However, it will be shown in Section 6 how charm fragmentation data at $\Upsilon(4S)$ (10.6 GeV) and Z^0 (91.2 GeV) energies cannot be described simultaneously within perturbation theory. Without a more specific understanding of the origin of this problem, it would appear premature to even attempt to relate rigorously the charm and bottom non-perturbative fragmentation functions.

The large-N (or $x \to 1$) limit involves the matching of perturbative and non-perturbative physics. In the case of the initial condition for the fragmentation function, the region where $(1-x)\,m \approx \Lambda$ (i.e. $m/N \approx \Lambda$ in moment space) is sensitive to the decay of excited states of the heavy-flavoured hadrons, and is thus controlled by non-perturbative physics. In the case of the coefficient functions, when $(1-x)Q^2 \approx \Lambda^2$, the mass of the recoil system approaches typical hadronic scales. In the present work, we do not attempt a rigorous formulation of the perturbative/non-perturbative matching problem and of the ensuing description of the non-perturbative terms.[5] We instead simply look for a formulation of the resummation prescription that

(i) is consistent with all known perturbative results,

(ii) yields physically acceptable results,

(iii) does not introduce power corrections larger than generally expected for the processes in question, i.e. $N\Lambda/m$ for the initial condition [23–25, 21] and $N\Lambda^2/q^2$ for the coefficient functions [26], where Λ is a typical hadronic scale of a few hundreds MeV.

---

[5]Such a rigorous separation has been investigated, for example, in ref. [22], in the framework of deep inelastic scattering.

In detail, as far as the coefficient function is concerned, we make the following replacement in eq. (2.31) (and hence (2.25) and (2.40))

$$N \to N \, \frac{1 + f/N_q^L}{1 + f \, N/N_q^L} \,, \tag{2.44}$$

where N_q^L is given in eq. (2.32) and f is a parameter not smaller than one, but of order one. For $N \ll N_q^L$, the replacement (2.44) amounts to a tower of power corrections to N, starting with $f(N-1)/N_q^L \approx f(N-1)\Lambda_{\mathrm{QCD}}^2/\mu^2$, consistently with items (i) and (iii) listed above. Furthermore, for large N, the replacement (2.44) becomes $N \to N_q^L/f$. Thus, with this replacement, the functions $g^{(1/2)}$ of eqs. (2.26) and (2.27) have no singularities in the half plane $\mathrm{Re}(N) > 0$, so that item (ii) above is also fulfilled.

For the initial condition, we apply the same prescription of eq. (2.44) in eq. (2.36) (and hence (2.33) and (2.41)), replacing N_q^L with N_{ini}^L (defined in eq. (2.37))

$$N \to N \, \frac{1 + f/N_{\mathrm{ini}}^L}{1 + f \, N/N_{\mathrm{ini}}^L} \,. \tag{2.45}$$

In this case, the replacement amounts to a tower of power corrections starting with $f(N-1)/N_{\mathrm{ini}}^L \approx f(N-1)\Lambda_{\mathrm{QCD}}/\mu_0$, and for large N the branch cut in eqs. (2.34) and (2.35) is never reached.

The Landau singularity is regulated if $f \geq 1$. For f below 1 the effect of the Landau pole should be visible. We plot in figure 1 the results of varying the f parameter ($f = 0$, i.e. no regulator, 0.5, 1 and 1.5), together with the pure perturbative result, without Sudakov resummation. First of all, we notice the tiny cusp due to the Landau singularities, located around $N \approx 7.2$, consistently with eq. (2.37). The moments become negative (and therefore unphysical) after the cusp. With increasing f, the cusp is displaced to larger values of N, until it disappears for $f = 1$. The fixed order cross section also changes sign at $N \approx 11$, larger than N_{ini}^L. This is consistent with the large N behaviour of $d_Q^{(1)}$ shown in eq. (2.22), such that $D_Q(N)$ becomes negative when

$$N \approx \exp \sqrt{\frac{\pi}{C_{\mathrm{F}}\alpha_{\mathrm{S}}(m^2)}} \,. \tag{2.46}$$

However, for small enough α_{S}, this value should be parametrically smaller than N_{ini}^L. In the case of charm production, this does not happen, reminding us that we are at the limit of validity of perturbation theory. A more consistent behaviour is observed in the bottom case, figure 2. In this figure, the pattern of improvement towards the large-N region, when going from the purely-perturbative initial condition without soft gluon resummation, to the inclusion of soft-gluon effects, and then to the addition of the non-perturbative regularization, is clearly visible.

We conclude our discussion with the following remarks. We have found that, while for bottom production the NLO result, the inclusion of Sudakov effects and the regularization of the Landau singularities follow numerically the correct pattern of improvements, in the case of charm production the inclusion of Sudakov effects induces a worse large-N behaviour
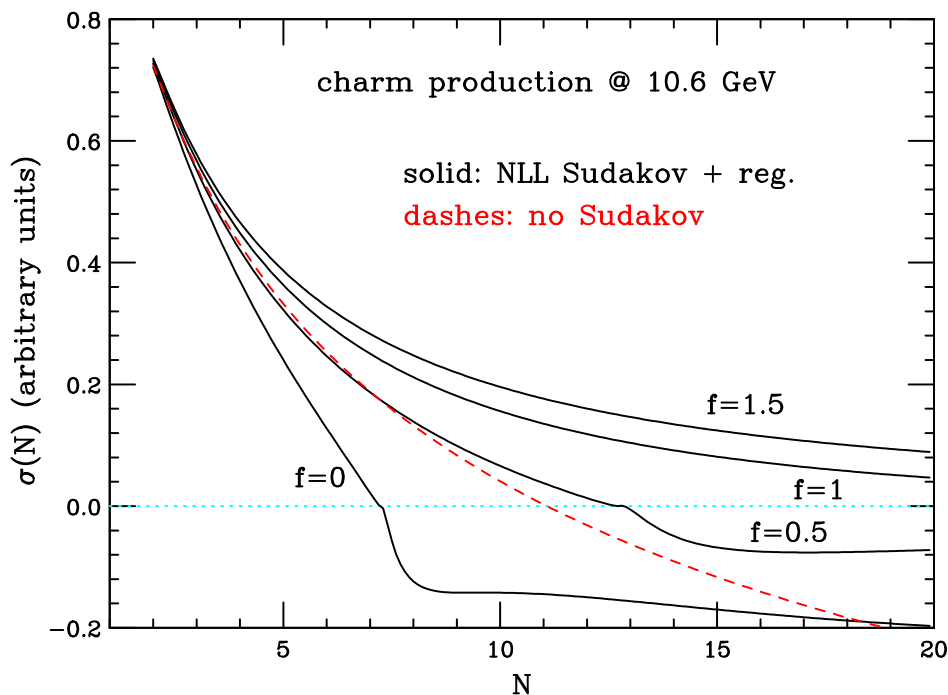
Figure 1: Moments of the perturbative fragmentation function for charm production at $\sqrt{q^2} = 10.6$ GeV with and without soft-gluon resummation with different values of f, eqs. (2.44) and (2.45), in the regularization of the Landau pole singularities.
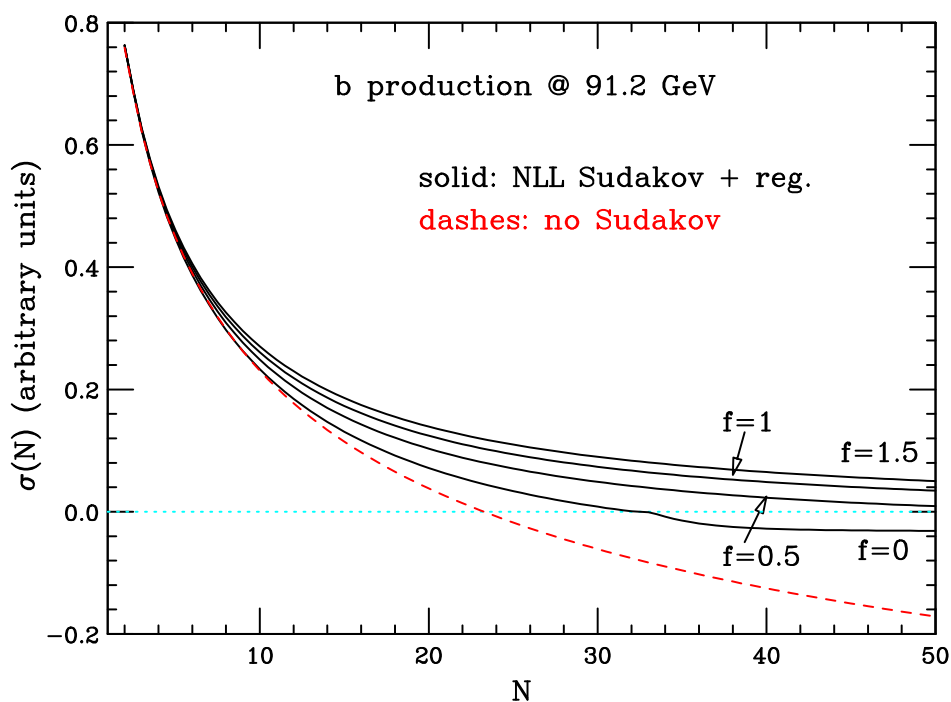
Figure 2: As in figure 1 for bottom production at $\sqrt{q^2} = 91.2$ GeV.

of the cross section, signaling the imperfect applicability of perturbation theory in this case. Nevertheless, in both cases we have shown that we can obtain a sensible physical result with formulae that are consistent with all known results in perturbative QCD, and modest power suppressed effects according to the item (iii). We will thus apply our procedure to the fits of charm and bottom data. We will use the value $f = 1.25$ in our fits, since we found that good fits can be obtained with this choice. We remark that the parameters of the non-perturbative fragmentation function that we obtain in our fits do depend upon the choice of f, to an extent that can be inferred from Figs. 1 and 2. It is also clear that, for moments around $N \approx 5$, the effect of the inclusion of a regulated Sudakov is modest. We will discuss in Section 8 the implications of this fact for hadronic cross sections.

2.4 The bottom threshold

In analogy with parton distribution functions, also parton fragmentation functions obey matching conditions when crossing heavy-flavour thresholds. In ref. [10], we have computed these matching conditions at next-to-leading order in the strong coupling constant α_S in the $\overline{\mathrm{MS}}$ scheme. We obtain, neglecting $\mathcal{O}(\alpha_\mathrm{S}^2)$ corrections

$$D_{Q/\bar{Q}}^{(n_\mathrm{f})}(x, \mu_\mathrm{thr}^2, m_\mathrm{thr}^2) = \int_x^1 \frac{dy}{y}\, D_g(x/y, \mu_\mathrm{thr}^2, m_\mathrm{thr}^2)$$
$$\times \frac{\alpha_\mathrm{S}}{2\pi}\, C_\mathrm{F}\, \frac{1 + (1-y)^2}{y} \left[\log \frac{\mu_\mathrm{thr}^2}{m_\mathrm{thr}^2} - 1 - 2\log y\right] \qquad (2.47)$$

$$D_g^{(n_\mathrm{f})}(x, \mu_\mathrm{thr}^2, m_\mathrm{thr}^2) = D_g^{(n_\mathrm{L})}(x, \mu_\mathrm{thr}^2, m_\mathrm{thr}^2)\left(1 - \frac{T_\mathrm{F}\alpha_\mathrm{S}}{3\pi} \log \frac{\mu_\mathrm{thr}^2}{m_\mathrm{thr}^2}\right) \qquad (2.48)$$

$$D_{i/\bar{i}}^{(n_\mathrm{f})}(x, \mu_\mathrm{thr}^2, m_\mathrm{thr}^2) = D_{i/\bar{i}}^{(n_\mathrm{L})}(x, \mu_\mathrm{thr}^2, m_\mathrm{thr}^2) \qquad \text{for } i = q_1, \dots q_{n_\mathrm{L}} \ , \qquad (2.49)$$

where $n_\mathrm{L} = n_\mathrm{f} - 1$ is the number of light flavours. Since, in the present paper, we are interested in the evolution of charm fragmentation function from lower scales, of the order of the charm mass, to higher scales, these matching conditions should be used for consistency when crossing the bottom threshold.

In this framework, at low energies (i.e. not much above the charm mass), the charm is treated as a heavy quark, in order to provide a perturbative expression for its fragmentation function. Near the bottom threshold, the bottom is treated as heavy, while all other quarks (including charm) are considered light.

2.5 Simplified evolution scheme

For the phenomenological analysis performed in the present work, we have numerically solved the full set of evolution equations. It turns out, however, that, for the case of charm production at $\Upsilon(4S)$ energies, the contribution coming from gluon-splitting processes is fully negligible. Our results, in this case, can thus be obtained in a simplified framework, where only the P_{qq} splitting function is kept. The Mellin transform of P_{qq} can be performed analytically, and one can work with n_L flavours, since the annihilation energy is of the order

of the bottom mass. The evolution equation has the simple solution

$$E(N, \mu^2, \mu_0^2) = \exp \left\{ \log \frac{\alpha_{\mathrm{s}}(\mu_0^2)}{\alpha_{\mathrm{s}}(\mu^2)} \frac{P_{qq}^{(0)}(N)}{2\pi b_0} \right.$$
$$\left. + \frac{\alpha_{\mathrm{s}}(\mu_0^2) - \alpha_{\mathrm{s}}(\mu^2)}{4\pi^2 b_0} \left[P_{qq}^{(1)}(N) - \frac{2\pi b_1}{b_0} P_{qq}^{(0)}(N) \right] \right\}. \qquad (2.50)$$

Our final formula for the cross section, neglecting singlet contributions, is then, using eqs. (2.42), (2.43) and (2.50)

$$\sigma_Q(N, q^2, m^2) = C_q^{\mathrm{res}}(N, q^2, \mu^2) \, E(N, \mu^2, \mu_0^2) \, D_Q^{\mathrm{res}}(N, \mu_0^2, m^2). \qquad (2.51)$$

The Mellin transforms for $a_q^{(1)}$, $d_Q^{(1)}$ and $P_{qq}^{(1)}$ are given in formulae (A.12), (A.13) and (A.20) of ref. [1].[6]

3. Electromagnetic initial-state radiation

Electromagnetic initial-state radiation (ISR) can significantly affect the single-inclusive distribution of charmed mesons. At CLEO and BELLE energies, the hadronic cross section decreases as the inverse of the squared mass of the hadronic system. Initial-state photon radiation is suppressed by a factor of α_{em}, enhanced by a $\log s/m_e^2$ (m_e being the electron mass), and, depending upon how much energy is radiated away, due to the lower hadronic mass, it is enhanced by a larger hadronic cross section. The shape of the fragmentation function is also affected, since a consistent fraction of events takes place at lower hadronic invariant mass. CLEO and BELLE do not correct their data for initial-state radiation, so, in order to perform a meaningful fit to the fragmentation function, we have to take it into account.

We correct the initial distributions of measured inclusive cross sections bin by bin, i.e. we find, by an iterative procedure, a new distribution that reproduces the measured one after ISR has been implemented. More specifically: calling x_i, $i = 1, \ldots n$, the centre of the bins of the experimental distribution, we find a distribution $D_c(x)$ (where the suffix c stands for "corrected") that is continuous, vanishes at $x = 0$ and $x = 1$, and is linear in all intervals $(0, x_1), (x_1, x_2), \ldots, (x_{n-1}, x_n), (x_n, 1)$, such that, when ISR corrections are applied, we reproduce the measured distribution.

We model ISR in the following way. We assume for the radiated electromagnetic energy the distribution [27–30]

$$\frac{dP}{dz} = \delta \beta (1 - z)^{\beta - 1} - \frac{\beta}{2}(1 + z), \qquad (3.1)$$

where

$$\beta = 2 \frac{\alpha_{\mathrm{em}}}{\pi} \left[\log \frac{s}{m_e^2} - 1 \right], \quad \delta = 1 + \frac{3}{4}\beta + \frac{\alpha_{\mathrm{em}}}{\pi} \left(\frac{\pi^2}{3} - \frac{1}{2} \right), \quad z = \frac{s_{\mathrm{had}}}{s}, \qquad (3.2)$$

---

[6]We point out that there is an obvious misprint in ref. [1], where formula (A.7) should be replaced by

$$\psi_m(x) = \frac{d^{m+1} \log \Gamma(x)}{dx^{m+1}}.$$

$s = q^2$ being the squared centre-of-mass (CM) energy, and s_{had} the square of the invariant hadronic mass. The kinematic distribution of the hadronic system is assumed to be as if only a single photon, collinear to either the electron or the positron, was radiated. This assumption neglects double radiation, which gives effects of the order β^2, and the transverse momentum of the radiated photon, which is typically much smaller than the available energy. We use the Born cross section for the heavy-quark production in the hadronic reference frame. The value of x in the laboratory frame is obtained by a Lorentz boost. In summary

$$D(x_i) = \int_{\frac{4m_h^2}{s}}^1 dz \int dy \, d\cos\theta \, \frac{1}{\sigma_0(s)} \frac{d\sigma_0(zs, \cos\theta)}{d\cos\theta} \frac{dP}{dz} D_c(y) \, \delta(x_i - x(z, y, \theta)) \,, \qquad (3.3)$$

where $x(z, y, \theta)$ is the momentum fraction of the heavy flavoured hadron (of mass m_h) in the e^+e^- CM frame. It is obtained as follows. We define the momentum components of the hadron in the hadronic CM system

$$p_h = \frac{y}{2}\sqrt{sz - 4m_h^2}\,, \qquad p_h^0 = \sqrt{p_h^2 + m_h^2}\,, \qquad p_h^{\parallel} = p_h \cos\theta \,, \qquad (3.4)$$

so that y is its momentum fraction. Then we boost it to the e^+e^- CM frame. Under our assumptions (that all the electromagnetic energy is collinear either to the electron or to the positron, and that double radiation and the photon transverse momentum are negligible) the boost velocity is purely longitudinal, and is given by $v = (1 - z)/(1 + z)$. The hadron momentum in the e^+e^- CM frame is then

$$p^0 = \frac{p_h^0 + v p_h^{\parallel}}{\sqrt{1 - v^2}}\,, \qquad p = \sqrt{p_0^2 - m_h^2}\,, \qquad (3.5)$$

and

$$x(z, y, \theta) = \frac{p}{\sqrt{s/4 - m_h^2}}\,. \qquad (3.6)$$

We use for σ_0 the exact Born cross section in the massless limit. Since asymmetries cancel in eq. (3.3), we always assume the angular dependence

$$\frac{1}{\sigma_0(s)} \frac{d\sigma_0(zs, \cos\theta)}{d\cos\theta} = \frac{\sigma_0(zs)}{\sigma_0(s)} \frac{3}{8} \left(1 + \cos^2\theta\right) \,. \qquad (3.7)$$

We do, however, supply the threshold factor to the total cross section. Thus, near the $\Upsilon(4S)$ we have

$$\frac{\sigma_0(zs)}{\sigma_0(s)} = \frac{\theta(zs - 4m_h^2)}{z} \frac{\left(1 + \frac{2m^2}{sz}\right)\sqrt{1 - \frac{4m^2}{sz}}}{\left(1 + \frac{2m^2}{s}\right)\sqrt{1 - \frac{4m^2}{s}}}\,. \qquad (3.8)$$

We checked that the effect of finite mass corrections to the angular distribution, the use of m_h instead of the quark mass m in the threshold factor, as well as the scaling violations in the fragmentation function due to the reduced (i.e. $s \to sz$) CM hadronic energy, have a negligible impact on our results.
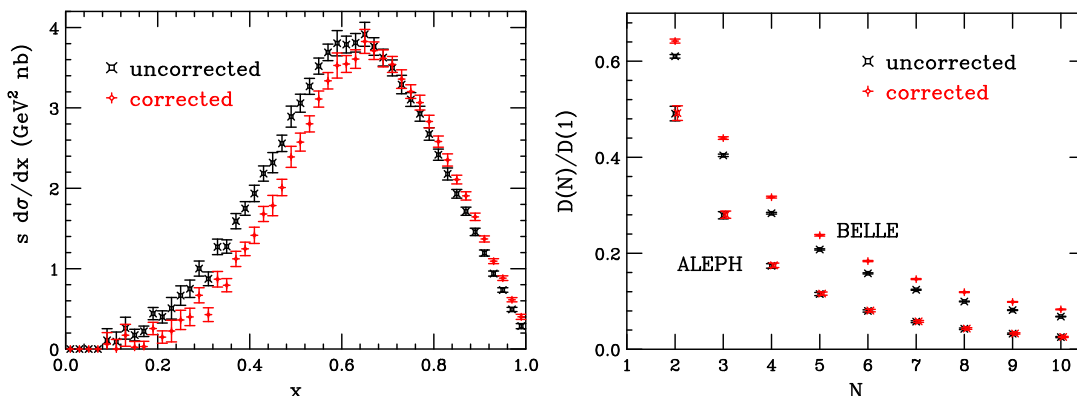
Figure 3: Left: the effect of the ISR correction on BELLE data for $D^{*+} \to D^0 \pi^+$. Right: the same data in moment space, shown together with the ALEPH ones.

The effect of the ISR correction is displayed in figure 3, where BELLE data for $D^{*+} \to D^0 \pi^+$ are displayed before and after the ISR correction has been applied, both in x and moment space. The ALEPH data are also shown in moment space. We see that the corrected spectrum for BELLE is harder and lower in normalization than the uncorrected one. This is to be expected, since ISR lowers the available hadronic energy, thus softening the spectrum and increasing the cross section at the same time. We can also see that the effect for BELLE is not large, but nonetheless not negligible. It is instead much less prominent, up to the point of being negligible, for the ALEPH data taken on the Z^0 peak, as expected.

4. Non-perturbative fragmentation function

In the heavy-quark fragmentation-function formalism, the largest non-perturbative effects come from the initial condition, since one expects power corrections of the form Λ/m. We assume that all these effects can be described by a non-perturbative fragmentation function D_{NP}, that takes into account all low-energy effects, including the process of the heavy quark turning into a heavy-flavoured hadron, that has to be convoluted with the perturbative cross section. Thus, the Mellin transform of the full resummed cross section, including non-perturbative corrections, is

$$\sigma_H(N, q^2) = \sigma_Q(N, q^2, m^2) D_{\mathrm{NP}}(N) \,. \tag{4.1}$$

We have attempted to fit CLEO and BELLE D^* data using several forms for D_{NP}. We found that the best fits are obtained with the two-component form

$$D_{\mathrm{NP}}(x) = \mathrm{Norm.} \times \frac{1}{1+c} \left[\delta(1-x) + c N_{a,b}^{-1} (1-x)^a x^b \right] \,, \tag{4.2}$$

with

$$N_{a,b} = \int_0^1 (1-x)^a x^b \,. \tag{4.3}$$

This form is a superposition of a maximally hard component (i.e. the delta function) and the form proposed in ref. [31]. It can be given a simple phenomenological interpretation, the hard term corresponding in some sense to the direct exclusive production of the D^*, and the Colangelo-Nason form accounting for D^*'s produced in the decay chain of higher resonances.

Following the approach of ref. [32], we assume that the D meson non-perturbative fragmentation function is the sum of a direct component, which is isospin invariant, plus the component arising from the D^* decay. The decay $D^* \to D\pi$ is very close to threshold, so that the D has the same velocity of the D^*, and their momenta are thus proportional to their masses. Under these circumstances, the component of the D fragmentation function arising from $D^* \to D\pi$ decays is given by

$$B(D^* \to D\pi) \, \tilde{D}_\pi^D(x) \,, \tag{4.4}$$

where we have defined

$$\tilde{D}_\pi^D(x) = D_{\mathrm{NP}}^{D^*}\left(x \frac{m_{D^*}}{m_D}\right) \frac{m_{D^*}}{m_D} \, \theta\left(1 - x\frac{m_{D^*}}{m_D}\right) \,, \tag{4.5}$$

and $B(D^* \to D\pi)$ is the branching ratio of $D^* \to D\pi$. Observe that $\tilde{D}_\pi^D$ has been defined so as to have the same normalization as $D_{\mathrm{NP}}^{D^*}$. In N space we obtain immediately

$$\tilde{D}_\pi^D(N) = D_{\mathrm{NP}}^{D^*}(N) \left[\frac{m_D}{m_{D^*}}\right]^{N-1} \,. \tag{4.6}$$

For the $D^* \to D\gamma$ decay, in the D^* frame, the D has non-negligible velocity, but it is non-relativistic. We call θ its decay angle with respect to the D^* direction, and p_D its momentum

$$p_D = \frac{m_{D^*}^2 - m_D^2}{2m_{D^*}} \,. \tag{4.7}$$

We call β the D^* velocity and $\gamma = 1/\sqrt{1 - \beta^2}$. Thus, the longitudinal component of the D momentum in the laboratory frame is given by a Lorentz boost

$$\gamma\left(p_D \cos\theta + \beta m_D\right) \,, \tag{4.8}$$

where we have neglected terms of order p_D^2. Thus the component of the D fragmentation function coming from $D^* \to D\gamma$ decay is given by

$$B(D^* \to D\gamma) \, \tilde{D}_\gamma^D(x) \,, \tag{4.9}$$

with

$$\tilde{D}_\gamma^D(x) = \int dy \, \frac{d\cos\theta}{2} \, D_{\mathrm{NP}}^{D^*}(y) \, \delta\left(\frac{\gamma(p_D \cos\theta + \beta m_D)}{p_{\max}} - x\right) \,, \tag{4.10}$$

where $p_{\max}$ is the maximum D momentum in the laboratory. Since we always consider the ultra relativistic limit, we have

$$y = \frac{\gamma m_{D^*}}{p_{\max}} \,, \quad \beta \to 1 \,, \tag{4.11}$$

D (mass in GeV)	branching ratios
$D^{*0}(2006.7 \pm 0.4) \rightarrow D^0\pi^0$	0.619 ± 0.029
$\rightarrow D^0\gamma$	0.381 ± 0.029
$D^{*+}(2010.0 \pm 0.4) \rightarrow D^0\pi^+$	0.677 ± 0.005
$\rightarrow D^+\pi^0$	0.307 ± 0.005
$\rightarrow D^+\gamma$	0.016 ± 0.004
$D^0(1864.5 \pm 0.4) \rightarrow K^-\pi^+$	0.0381 ± 0.0009
$D^+(1869.3 \pm 0.4) \rightarrow K^-\pi^+\pi^+$	0.092 ± 0.006

Table 1: Charm hadron masses and branching ratios.

so that we obtain

$$\tilde{D}_\gamma^D(x) = \int dy \, \frac{d\cos\theta}{2} \, D_{\rm NP}^{D^*}(y) \, \delta\left(\frac{y(p_D \cos\theta + m_D)}{m_{D^*}} - x \right) . \qquad (4.12)$$

The double integral cannot be performed in closed form. However, it is easy to obtain the moments

$$\tilde{D}_\gamma^D(N) = D_{\rm NP}^{D^*}(N) \int \frac{d\cos\theta}{2} \left[\frac{p_D \cos\theta + m_D}{m_{D^*}} \right]^{N-1}$$

$$= D_{\rm NP}^{D^*}(N) \frac{m_{D^*}}{2p_D} \frac{(m_D + p_D)^N - (m_D - p_D)^N}{N m_{D^*}^N} . \qquad (4.13)$$

We thus describe $D^{+/0}$ production as the sum of a primary (i.e. not coming from D^* decays) component, plus the contributions coming from D^* decays

$$D_{\rm NP}^{D^+}(x) = D_{\rm NP}^{D^+,p}(x) + B(D^{*+} \rightarrow D^+\pi^0)\tilde{D}_\pi^{D^+}(x)$$
$$+ B(D^{*+} \rightarrow D^+\gamma)\tilde{D}_\gamma^{D^+} D(x) , \qquad (4.14)$$

$$D_{\rm NP}^{D^0}(x) = D_{\rm NP}^{D^0,p}(x) + [B(D^{*+} \rightarrow D^0\pi^+) + B(D^{*0} \rightarrow D^0\pi^0)]\tilde{D}_\pi^{D^0}(x)$$
$$+ B(D^{*0} \rightarrow D^0\gamma)\tilde{D}_\gamma^{D^0}(x) . \qquad (4.15)$$

We took the value of masses and branching ratios from ref. [33]. For reference, we report in table 1 the values we used for the masses and for the decay rates of the charmed mesons.

5. D mesons data fits near the $\Upsilon(4S)$

Several parameters enter our calculations. First of all, at all matching points, there are scale choices that could be varied, to yield a perturbative uncertainty in our result. Those are the initial evolution scale μ_0, the matching scale for the crossing of the b threshold $\mu_{\rm thr}$, and the final evolution scale μ. In the present work we fix

$$\mu_0 = m , \quad \mu = \sqrt{q^2} , \quad \mu_{\rm thr} = m_{\rm thr} = m_b . \qquad (5.1)$$

These scales could, in principle, be varied by a factor of order two around the values listed above, yielding a sensibly different result. However, in general, the scale variation

Eq. (4.2): $a = 1.8 \pm 0.2$, $b = 11.3 \pm 0.6$, $c = 2.46 \pm 0.07$, total $\chi^2 = 139$				
Set	(C) D^{*+}	(B) $D^{*+} \to D^0$	(B) $D^{*+} \to D^+$	(C) D^{*0}	(B) D^{*0}
Norm.	0.238	0.253	0.227	0.225	0.211
χ^2/pts	33/16	63/46	13/46	13/16	17/46

Table 2: Results of the fit to D^* CLEO (C) and BELLE (B) data. The last line reports the χ^2 over the number of fitted points for each data set.

will simply result in different values for the fitted parameters of the non-perturbative form. When computing cross sections for different processes, one should then use the parametrization appropriate for the scale choice that has been made in the fit, hence compensating for the change. In the present work we will not pursue this issue further, since our aim is simply to show that a fit within QCD is possible. A similar remark applies to the value of Λ_{QCD} and the quark masses, that we will fix at

$$\Lambda_{\text{QCD}}^{(5)} = 0.226 \text{ GeV}, \quad m_c = 1.5 \text{ GeV}, \quad m_b = 4.75 \text{ GeV}. \tag{5.2}$$

The CLEO and BELLE data are given as absolute cross sections. Since we correct the data for ISR effects, we should normalized our data to the e^+e^- charm cross section corrected for ISR effects. We thus use the value of $R(e^+e^-)$ reported in ref. [34], defining

$$\sigma_c(s) = \sigma_{\mu^+\mu^-}^{(0)}(s) \times 3.56 \times 0.4 \times 2, \tag{5.3}$$

where $\sigma_{\mu^+\mu^-}^{(0)}(s) = 86.86 \text{ nb }/s$ is the Born cross section for $e^+e^- \to \mu^+\mu^-$, 3.56 is the value of R measured by CLEO, 0.4 is the charm fraction, and the factor of 2 allows for the counting of both charge conjugate states.

We have fitted all D^{*+} and D^{*0} data with the same set of parameters, except for the normalization, which is kept independent for each data set. This procedure is justified, since the errors in the data do not include overall errors that do not affect the shape of the fragmentation function. We have limited ourselves to the fit range $0.2 < x < 1$ for CLEO and $0.08 < x < 1$ for BELLE. In the case of BELLE data, we use only the continuum sample for $x < 0.5$, and for $x > 0.5$ we combine the continuum and the on-resonance sample in the following way

$$y = \frac{y_c/s_c^2 + y_r/s_r^2}{1/s_c^2 + 1/s_r^2}, \quad s = \frac{1}{\sqrt{1/s_c^2 + 1/s_r^2}}, \quad d = \frac{d_c/s_c^2 + d_r/s_r^2}{1/s_c^2 + 1/s_r^2}, \tag{5.4}$$

where $y_{c/r}$, $s_{c/r}$ and $d_{c/r}$ are the central value, the statistical error and the systematic error of the continuum/on-resonance data, and y, s and d are our combined central value, statistical error and systematic error. For all data sets we combine the statistical and systematic errors in quadrature.

The result of the fit is reported in table 2 and in figures 4–8 we show the data and the fitted curve, both in x and moment space.

A considerable part of D's are produced indirectly through D^* decays. Here we assume that both D^*'s and the D's that are not the product of D^* decay are produced with a
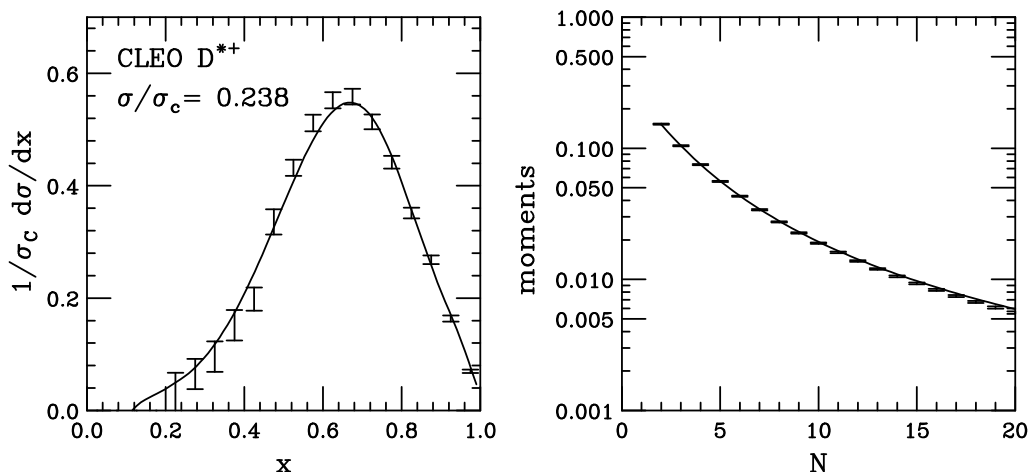
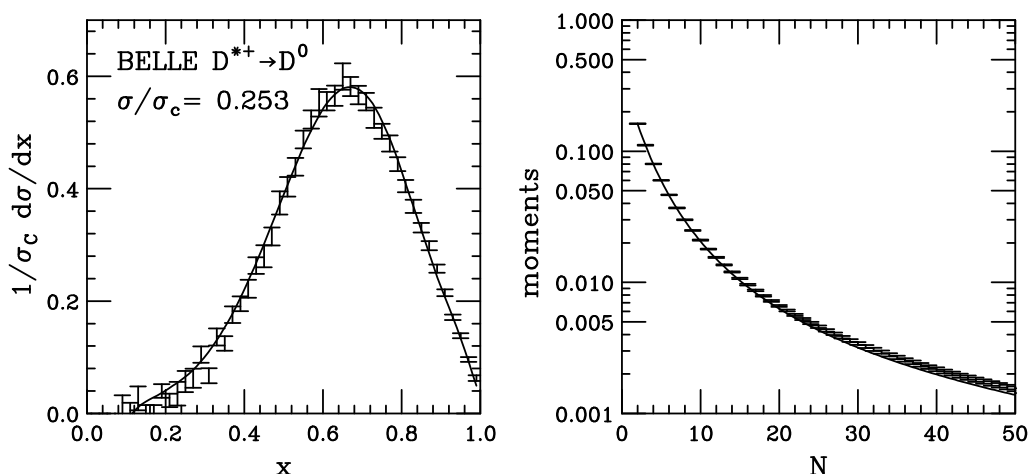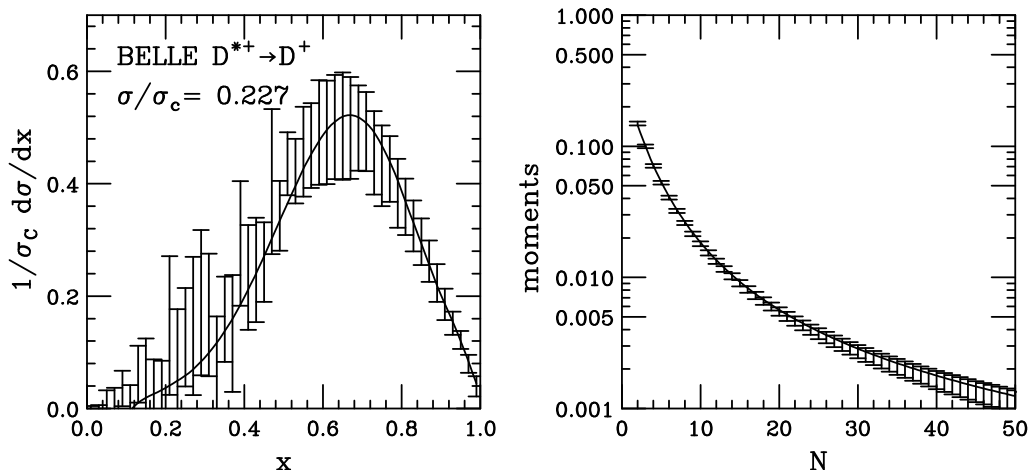**Figure 4:** Fit to CLEO D^{*+} data.

Figure 5: Fit to BELLE $D^{*+} \to D^0$ data.

charge-independent rate. Under this assumption, the fraction of "direct" (meaning not arising from D^*) and "indirect" (from D^*) D mesons are in relative proportion of 0.473 to 0.527. These numbers can be extracted from the total production cross section of charmed mesons reported in ref. [3], and from table IX of ref. [4]. We then use the parametrization of table 2 for the D^* production, the branching ratios for $D^* \to D$ decays given in table 1 and a description of the decay as detailed in Sec. 4.

We parametrize the direct D component with the same form used for the D^*, and fit it to the D^+ production data, where a larger fraction of direct D is expected. We then use the fitted direct D parametrization to describe the direct part of the D^0 production data. In all cases, the overall normalization is chosen for a best fit to each data set, in order to be insensitive to overall normalization differences.

The result of the fit for the $D^{+/0}$ mesons is reported in table 3. In figures 9–12 we show the data and the fitted curve, both in x and moment space.
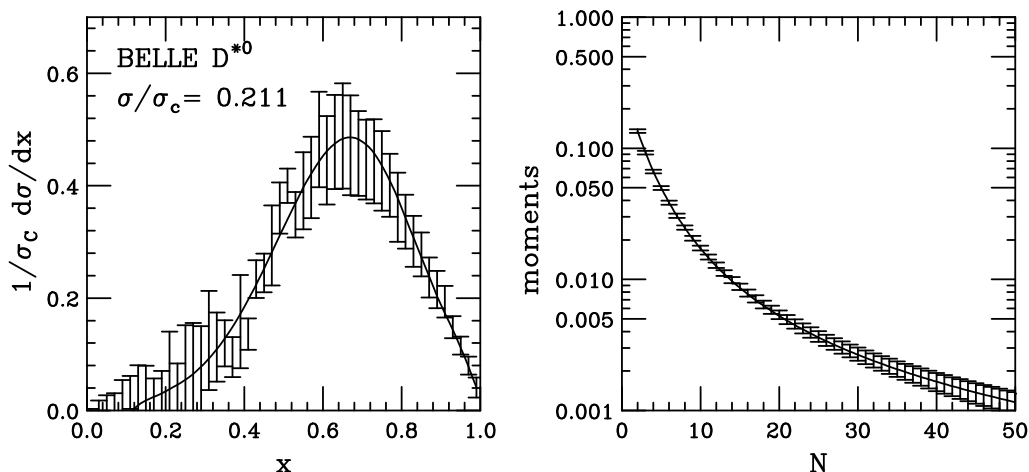
Figure 6: Fit to BELLE $D^{*+} \to D^+$ data.
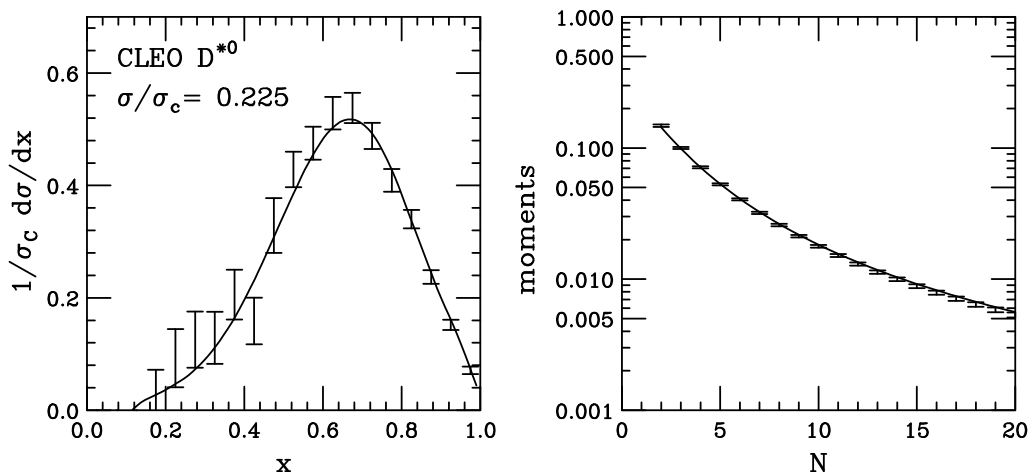
Figure 7: Fit to CLEO D^{*0} data.

Eq. (4.2): $a = 1.1 \pm 0.1$, $b = 7.6 \pm 0.6$, $c = 4.6 \pm 0.2$				
	total $\chi^2 = 50$		total $\chi^2 = 109$	
Set	(C) D^+	(B) D^+	(C) D^0	(B) D^0
Norm.	0.263	0.270	0.609	0.598
χ^2/pts	14/16	36/46	32/16	77/46

Table 3: Results of the fit to D CLEO (C) and BELLE (B) data. The fit was performed over the D^+ data only, that are more sensitive to the direct component, and then used to describe D^0 data.

6. D mesons data fits on the Z^0

In this work we use the data from the ALEPH collaboration [11], which are the most precise ones. These data are affected by electromagnetic initial-state radiation as well. However, unlike the $\Upsilon(4S)$ case, the ISR does not appreciably distort the spectrum, but it mostly affects the total cross section. This is easily understood: any appreciable amount of ISR on

Figure 8: Fit to BELLE D^{*0} data.
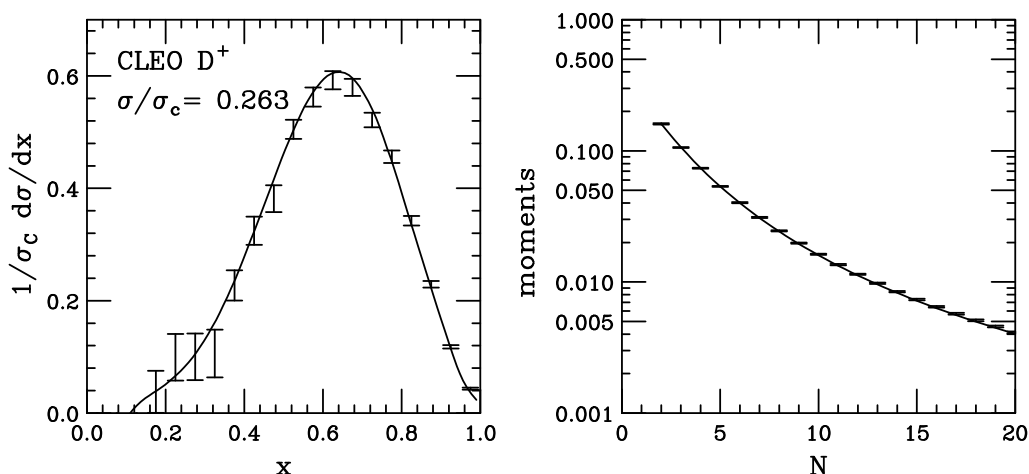
Figure 9: Fit to CLEO D^+ data.

the Z^0 peak brings the reaction off resonance, to a vanishing cross section. Thus, the bulk of heavy flavour production always takes place on the Z^0 peak. Conversely, at the $\Upsilon(4S)$ energy, the ISR generates processes with higher cross section and a lower hadronic invariant mass. Since the ALEPH data are normalized to the total number of hadronic events, the effects of ISR largely cancel in the ratio. We shall anyway perform the correction for ISR for these data as well.

In figure 13 we display our fit with ALEPH data. We fit the data in the region $x \in [0.4, 1]$ using the non-singlet component only, since a subtraction of the gluon-splitting contributions was performed by ALEPH. Observe that, in this calculation, the bottom-threshold crossing has to be dealt with, according to the discussion of Section 2.4. We also show, for comparison, the full evolution result (dashed line), using the same parameters obtained in the non-singlet fit. As we can see, the difference is only visible at small x. The
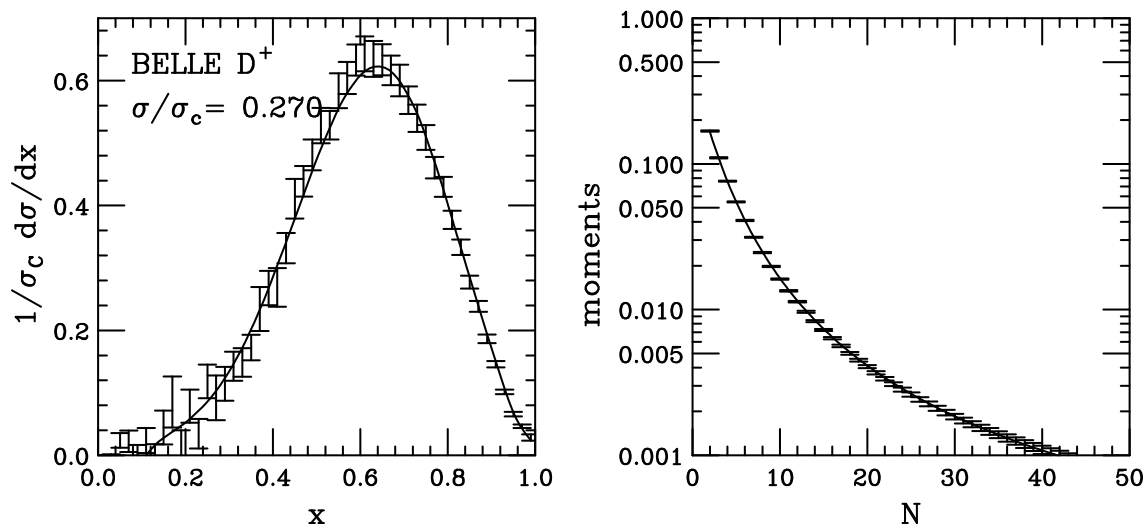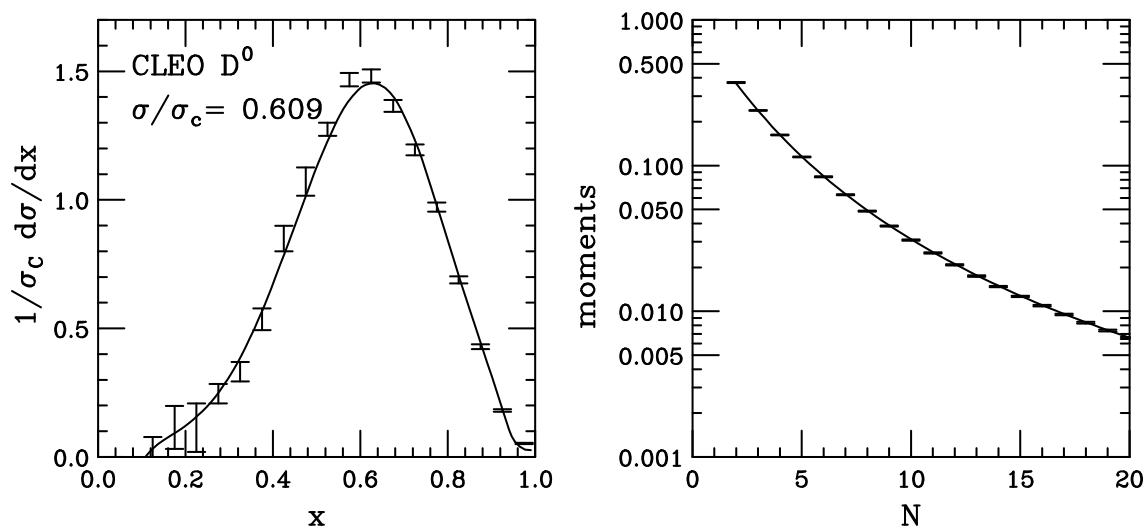
Figure 10: Fit to BELLE D^+ data.

Figure 11: CLEO D^0 data and the best fit extracted from D^+ data.

result of the fit for the non-perturbative parameters is

$$a = 2.4 \pm 1.2\,, \quad b = 13.9 \pm 5.7 \quad c = 5.9 \pm 1.7\,, \tag{6.1}$$

with a $\chi^2 = 4.2$ for 13 fitted points. These results are not really consistent with those for the $\Upsilon(4S)$ data in Tab. 2.

In order to better quantify the discrepancy between eq. (6.1) and table 2 we use the parametrization of CLEO and BELLE data to predict the D^* fragmentation function at LEP energies. The LEP prediction, using the parametrization of table 2, is reported in figure 14 together with ALEPH data. We observe that the fitted normalization is very close to the CLEO D^{*+} normalization. We find a $\chi^2 = 60.1$ (for 13 fitted points) for
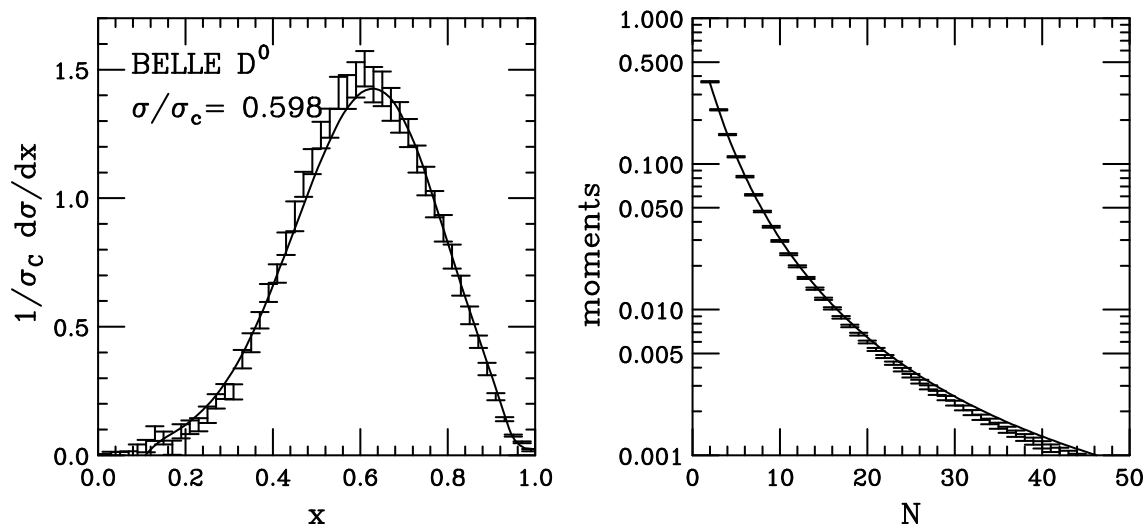
Figure 12: BELLE D^0 data and the best fit extracted from D^+ data.
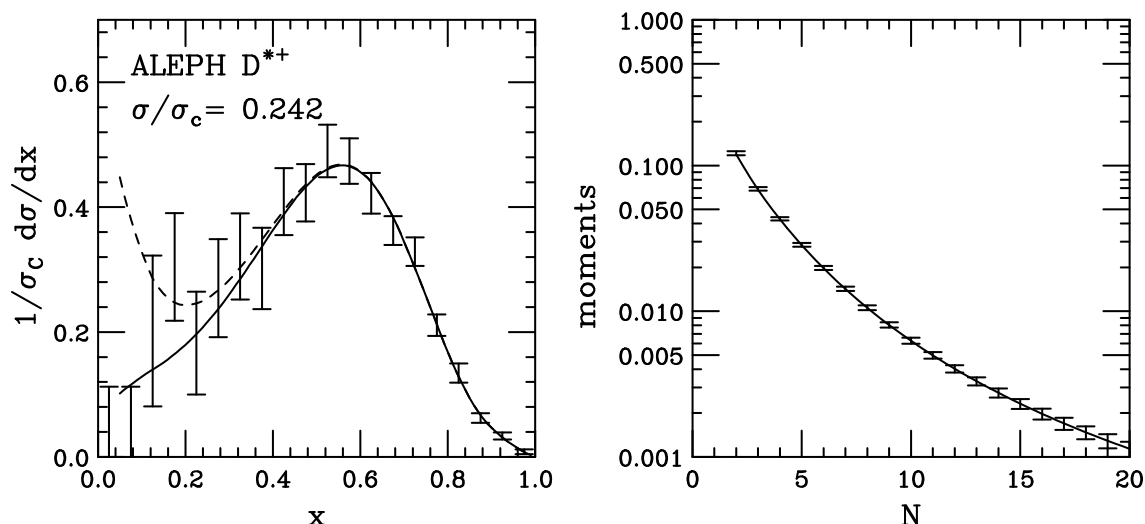
Figure 13: ALEPH D^{*+} data and the result of our non-singlet fit (solid line). The dashed line represents the result obtained using full evolution.

this parametrization. Thus, the description is not satisfactory, especially in the large-x (large-N) region.

In figure 15 we show the ratio of the moments of ALEPH D^{*+} data over our prediction. We observe that the N dependence of the ratio is well described by the functional form

$$\frac{1}{1 + 0.044\,(N-1)}, \tag{6.2}$$

where, since the first moment of the non-singlet distribution should be exactly given by the theory (because of charge conservation), we normalize to one the extrapolation of the data to $N = 1$.
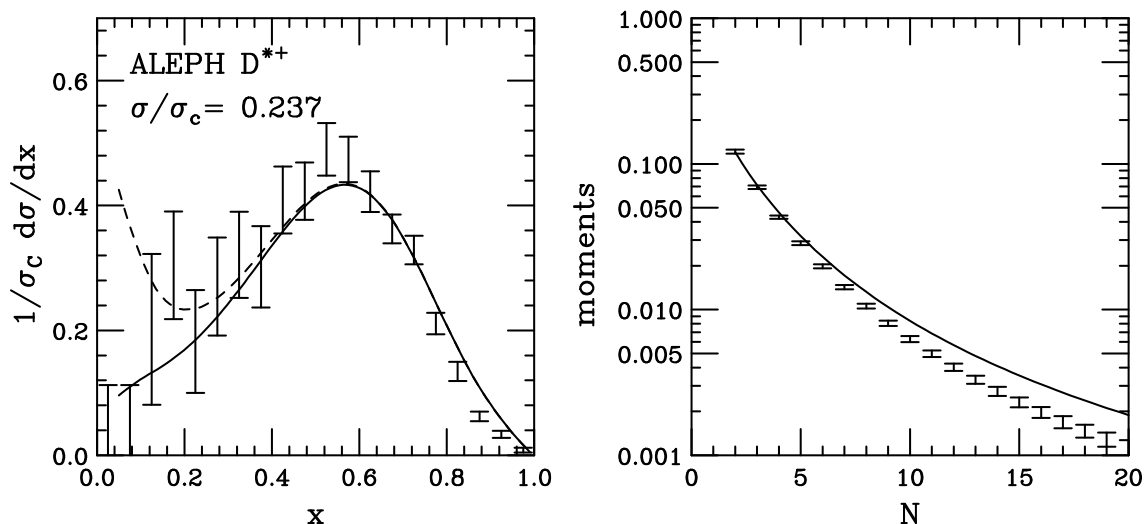
Figure 14: ALEPH D^{*+} data, compared to the QCD prediction.
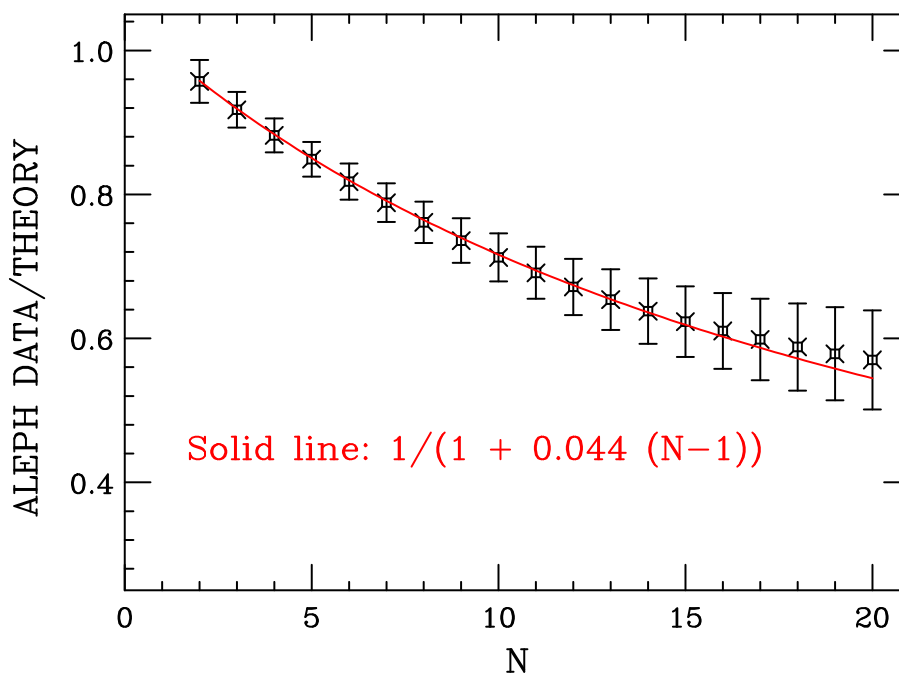

Solid line: $1/(1 + 0.044\ (N-1))$

Figure 15: ALEPH D^{*+} data, compared to the QCD prediction.

We can only speculate about the possible origin of the discrepancy and the form of the coefficient of $(N-1)$ in eq. (6.2). Assuming that we are dealing with a non-perturbative correction to the coefficient function of the form

$$1 + \frac{C(N-1)}{q^2},\tag{6.3}$$

this would lead to the extra factor

$$\frac{1 + \frac{C(N-1)}{M_Z^2}}{1 + \frac{C(N-1)}{M_\Upsilon^2}} \, , \tag{6.4}$$

(where M_Z and M_Υ are the Z^0 and $\Upsilon(4S)$ mass) to be applied to our prediction for the ALEPH data. For $C = 5$ GeV^2 we reproduce the behaviour of eq. (6.2). In ref. [26], on the basis of a calculation of infra-red renormalon effects, a $1/q^2$ power correction is found, with an N dependence marginally compatible with (6.3). No $1/E$ correction is found. ref. [35] also predicts a leading $1/E^2$ power correction. However, the $C \approx 5$ GeV^2 coefficient would appear to be somewhat too large.[7] Alternatively, if we admitted the existence of corrections to the coefficient functions of the form

$$1 + \frac{C(N-1)}{E} \, , \tag{6.5}$$

then we would find $C \approx 0.52$ GeV, a much more acceptable value. We observe that a form

$$\left(1 + \frac{C}{E}\right)^{N-2} \approx 1 + \frac{C(N-2)}{E} \tag{6.6}$$

was required in ref. [12] to fit light-hadron fragmentation data.

Demonstrating the absence (or the existence) of $1/E$ corrections in fragmentation functions would be a very interesting result, since it would help to validate or disprove renormalon-based predictions. Unfortunately, the low precision of the available data does not allow, at the moment, to resolve this issue.

We would like to remark that the discrepancy between the CLEO/BELLE and ALEPH data exclusively depends upon the evolution between the $\Upsilon(4S)$ and Z^0 energies. The method we used to describe the CLEO/BELLE data (i.e. the perturbative calculation of the fragmentation function, the Sudakov effects in the initial conditions and the parametrization of the non-perturbative part) does not affect the conclusions of the present section. In fact, we can simply compute the ratio of the moments of the inclusive D^{*+} (ISR corrected) distribution at CLEO/BELLE and ALEPH, and compare it to the theoretical prediction. The result of this comparison (where we have used, for simplicity, BELLE data only) is displayed in figure 16. The curves are given by

$$\frac{\sigma_Q(N, M_Z^2, m^2)}{\sigma_Q(N, M_\Upsilon^2, m^2)} = \frac{\bar{a}_q(N, M_Z^2, \mu_Z^2)}{1 + \alpha_s(\mu_Z^2)/\pi} \, E(N, \mu_Z^2, \mu_\Upsilon^2) \, \frac{1 + \alpha_s(\mu_\Upsilon^2)/\pi}{\bar{a}_q(N, M_\Upsilon^2, \mu_\Upsilon^2)} \tag{6.7}$$

where μ_Z and μ_Υ are the factorization scales and the evolution factor E is given in eq. (2.50). Notice that low-scale effects, both at the heavy quark mass scale and at the non-perturbative level, cancel completely in this ratio, making its prediction entirely perturbative. For $\bar{a}_q$, in the NLO results (dashed lines), we have used

$$\bar{a}_q(N, q^2, \mu^2) = 1 + \bar{\alpha}_s(\mu^2) \, a_q^{(1)}(N, q^2, \mu^2) \, , \tag{6.8}$$

---

[7]If we believe that it is the maximum meson energy, not E, that controls power effects, than we would have $C \approx 1$ GeV^2, a more acceptable value.
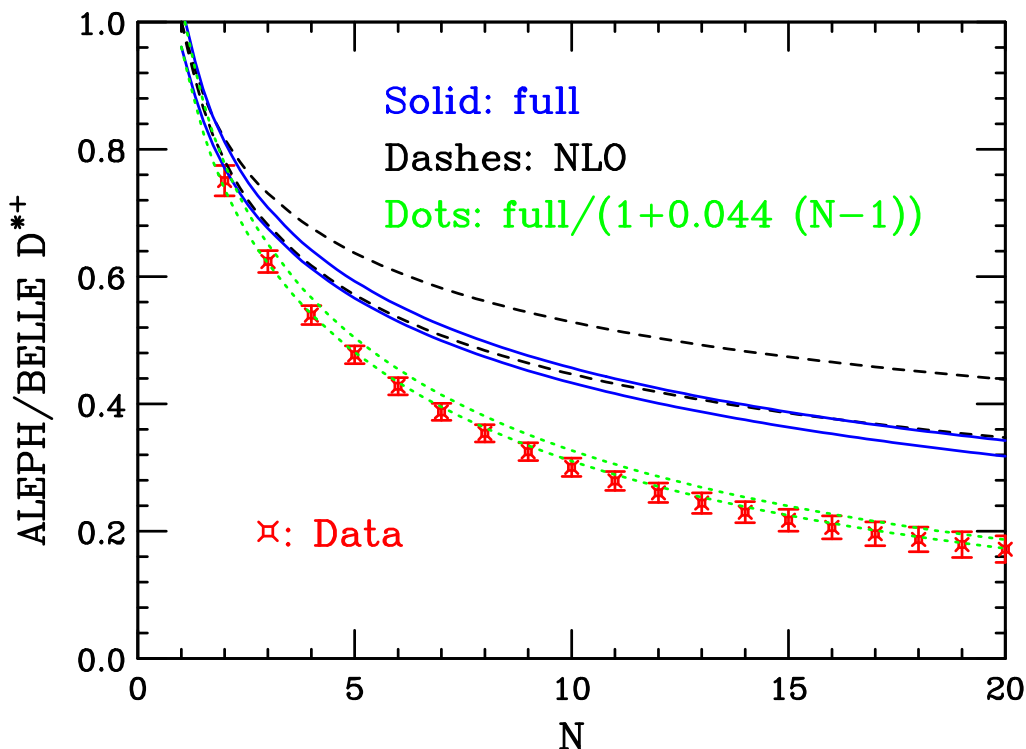
Figure 16: The ratio of ALEPH and BELLE moments for the D^{*+} fragmentation function, compared to QCD evolution. The solid band is obtained with QCD NLO evolution and Sudakov effects in the coefficient functions, while the dashed bands is NLO evolution only. The bands are obtained by setting $\mu_{Z/\Upsilon} = \xi M_{Z/\Upsilon}$ and varying $1/2 < \xi < 2$.

while for the full result (solid lines) we have included the NLL resummation of soft gluon emission in the coefficient functions

$$
\begin{aligned}
\bar{a}_q(N, q^2, \mu^2) &= \Delta_q^S(N, q^2, \mu^2) \\
&\times \left\{ 1 + \bar{\alpha}_s(\mu^2) \left[a_q^{(1)}(N, q^2, \mu^2) - \left[\Delta_q^S(N, q^2, \mu^2) \right]_{\alpha_S} \right] \right\}.
\end{aligned} \tag{6.9}
$$

The definitions of $a_q^{(1)}$ and Δ_q^S are given in Sections 2.1 and 2.2. We have set $\mu_{Z/\Upsilon} = \xi M_{Z/\Upsilon}$ with $\xi = 0.5, 2$ to plot our bands. As we can see from the figure, the rather large scale uncertainty displayed by the NLO result is much reduced when Sudakov effects are included. In both cases, however, the data clearly undershoot the pure QCD prediction, being instead compatible with the inclusion of the correction factor (6.2) (dotted lines). We have also checked that our full result is essentially unchanged if, instead of formula (6.9), we use the fully exponentiated formula (2.42). Furthermore, the change of variable given in eq. (2.44) to deal with the Landau pole has very little impact on our curves. Using the very large value $\Lambda_{\text{QCD}}^{(5)} = 0.3 \, \text{GeV}$ would lower the theoretical predictions by no more than 11% for $N \leq 20$, very far from explaining the observed effect.

The deconvolution of ISR effects, that hardens the $\Upsilon(4S)$ data, but is insignificant on the Z^0, widens the discrepancy. However, if we did not apply the deconvolution, the effect would still be partially visible.

Because of the relatively low energy of the data on the $\Upsilon(4S)$, it is legitimate to wonder whether charm-mass effects could be responsible for the discrepancy between LEP and $\Upsilon(4S)$ data. We have not included mass effects in the present calculation. However, in ref. [36], mass effects in charm production on the $\Upsilon(4S)$ where computed at order $\alpha_{\rm s}^2$, and found to be small (see figure 1 in the reference[8]).

We thus believe that it is unlikely that mass effects could play an important role in explaining this discrepancy.[9]

7. B mesons data fits on the Z^0

The same framework that yields good fits to D meson production data can also be used to describe B meson production on the Z^0. Accurate data have been published by the ALEPH [5], OPAL [6] and SLD [7] Collaborations. Preliminary data are available from DELPHI [8, 9]. We find that, to describe B production, the $\delta(1-x)$ term in eq. (4.2) is in fact not needed, i.e. the c parameter tends to become very large in the fitting procedure. In this limit the form of eq. (4.2) becomes a two parameter form, coinciding with that of ref. [31]. In figure 17 we show the result of a simultaneous fit to ALEPH and SLD data. In figure 18 we show the same best-fit curve together with the OPAL and DELPHI data. The fit yields $a = 24 \pm 2$, $b = 1.5 \pm 0.2$ with a $\chi^2 = 43$ for SLD and 51 for ALEPH for 21 and 19 data points respectively (for these data, bin-to-bin correlations provided by the experimental Collaboration were also taken into account). We did not attempt to fit the OPAL data together, since it was not clear to us how to handle the asymmetric, correlated systematic errors given by OPAL. However, it is clear from figure 18 that also this data set, as well as the preliminary data from DELPHI, is well described by the fit.[10]

8. Moment-space fits and power corrections

The fits presented so far have been performed on the measured x-space distributions, and they were aimed at providing an accurate description of all the experimental data. This has required a flexible parametrization for the non-perturbative fragmentation function, leading to the choice of the three-parameter form given in eq. (4.2). The data are fitted well in the large-x region, so that all moments of the fragmentation function are also well reproduced. This is important, since, as noted in refs. [37, 38], heavy-flavour production spectra in hadronic collisions are determined by a few Mellin moments (usually in the

---

[8]These results are given in x space. In the present work we have also computed the corresponding moment-space corrections at order $\alpha_{\rm s}$, and found effects of the order of 1% at $N = 5$, 4% at $N = 11$ and 7% at $N = 20$, very far from being able to explain the discrepancy.

[9]In refs. [23, 24], on the base of the analogy with the spacelike case, corrections of the form $\Lambda m/Q^2$ are introduced. Assessing the importance of these corrections in the present framework would require further investigation.

[10]Note that, while the ALEPH set refers specifically to B mesons, the SLD, DELPHI and OPAL data are for all weakly decaying b-flavoured hadrons. The two quantities could therefore be slightly different, due to the small fractions of B_s and B baryons (10% each, see ref. [33]). For an example of a quantitative estimate see eq. (5.10) of ref. [9].
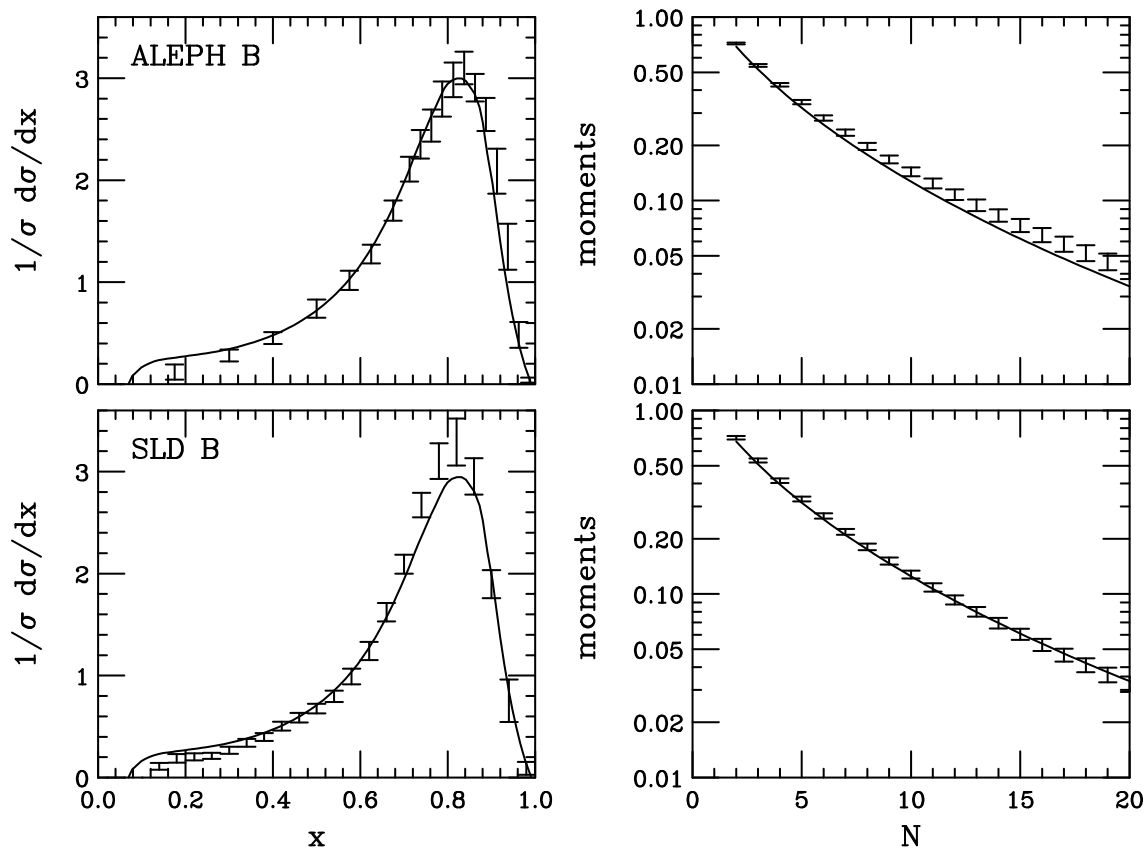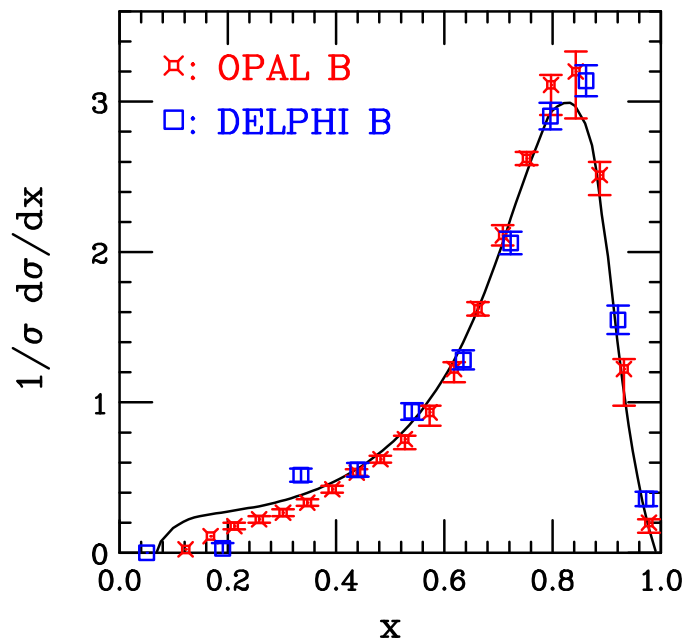
Figure 17: Fit of the fragmentation function for B production together with ALEPH (upper) and SLD (lower) data.
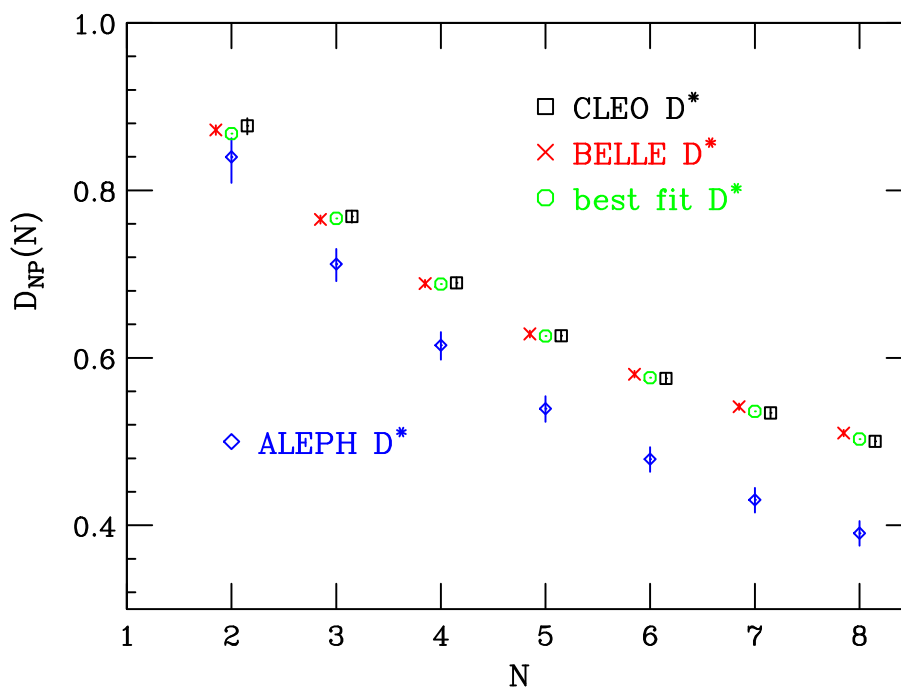
range $N = 2, \ldots 6$) of the non-perturbative fragmentation function. This property was successively exploited in refs. [39, 40, 32, 41] for predicting bottom and charm spectra in $p\bar{p}$ collisions. Inaccuracies in the description of the large-x region in e^+e^- annihilation could therefore lead to large errors in the moments that are relevant to the hadroproduction of heavy quarks. Conversely, in the framework of heavy-flavour production, an accurate fit in x-space is unnecessary, as long as the moments are well fitted in the relevant range. For this purpose, it is therefore convenient and sufficient to use for the non-perturbative fragmentation function one-parameter functional forms that are commonly found in the literature [42–44]. In the following discussion, we will focus upon these one-parameter forms, and in particular on the one of ref. [42]

$$D_{\mathrm{NP}}(x) = (\alpha + 1)(\alpha + 2)x^{\alpha}(1 - x). \tag{8.1}$$

It is important to stress that the choice of a specific parametrization like this one is exclusively a matter of convenience, aimed at easing the transfer of the non-perturbative information from e^+e^- collisions to other processes. One can either choose a different functional form, or even analyze the data in terms of non-perturbative moments $D_{\mathrm{NP}}(N)$ only.
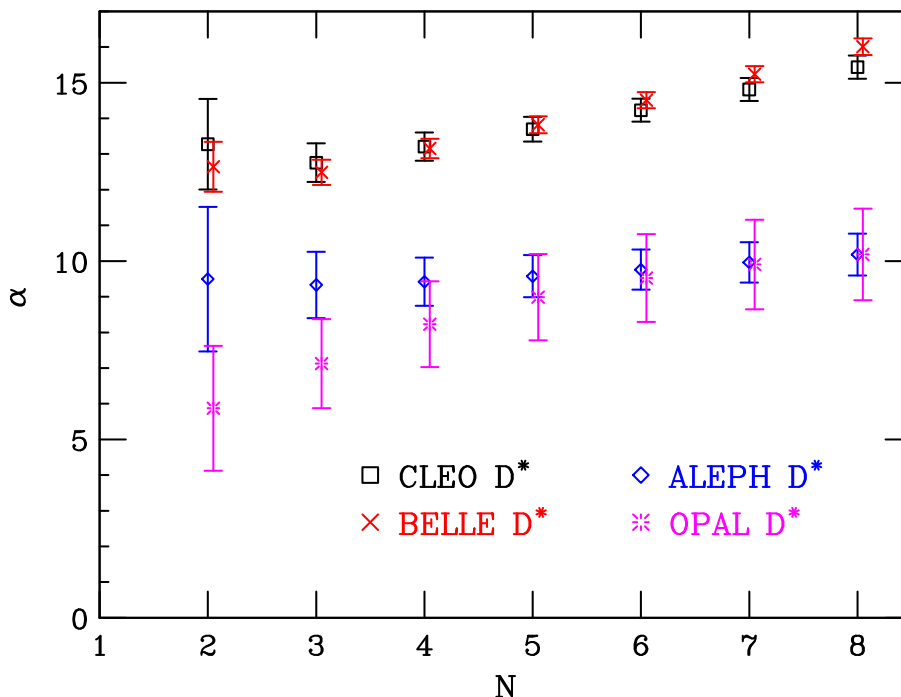
Figure 18: The fragmentation function fitted to ALEPH and SLD B data shown here together with OPAL and DELPHI data.

Figure 19: Moments of the non-perturbative component $D_{\mathrm{NP}}(N)$ extracted from e^+e^- D^* data, and those of the fitted non-perturbative fragmentation function (4.2) with the parameters of table 2.

In figure 19, we show the moments $D_{\mathrm{NP}}(N)$ extracted from e^+e^- data. The points in the figure are obtained by taking the experimental values of the moments of the fragmentation

Figure 20: Fits to D^{*+} data for the parameter α of the parametrization (8.1).

function together with their errors, divided by the pure perturbative component of the fragmentation function, computed with our default parameters.[11] In the figure we also show the non-perturbative component given by the form (4.2), with the parameters taken from table 2. Also evident is the poor consistency between values obtained from data taken on the $\Upsilon(4S)$ and on the Z^0. This is, of course, the same situation already observed in Section 6.

Using the Mellin transform of formula (8.1)

$$D_{\rm NP}(N) = \frac{(\alpha + 1)(\alpha + 2)}{(\alpha + N)(\alpha + N + 1)} \, , \tag{8.2}$$

we can translate the moments in figure 19 into values for α with the appropriately propagated error. The results are displayed in figure 20. From the figure we see that the one-parameter form (8.1) does not describe perfectly the whole shape, as shown by the non-constancy of α extracted from different moments. However, to a good degree of approximation a single value of α can describe all the moments up to $N \simeq 6$ or so. This is enough for the purpose of using the fitted function for convoluting a p_T distribution in hadronic collisions.

8.1 Scaling property: from D to B mesons

Several theoretical arguments in refs. [23 – 25, 21] predict for the heavy-quark non-perturbative

---

[11]The perturbative fragmentation function for ALEPH is computed using the non-singlet component only, since gluon-splitting contributions have been subtracted from the published experimental distribution.
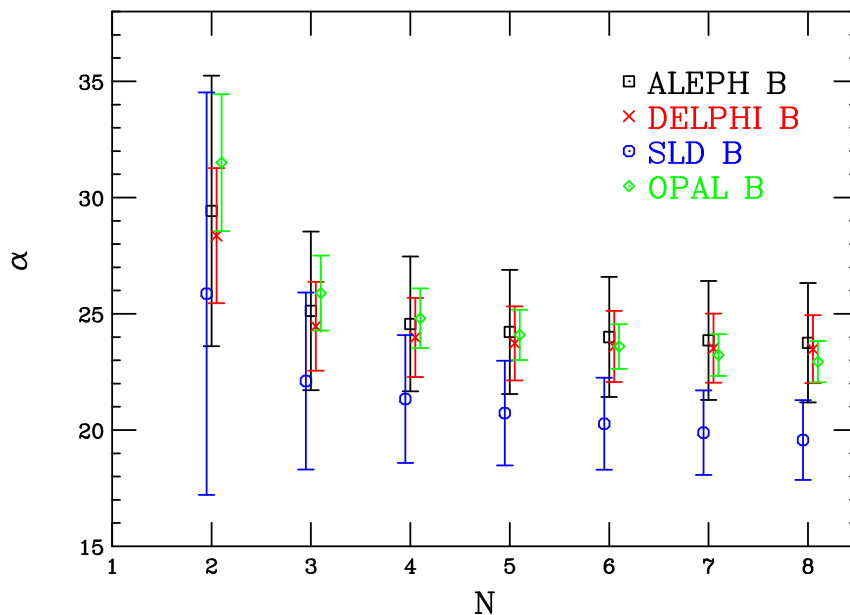
Figure 21: Fits to weakly decaying B's data for the parameter α of the parametrization of ref. [42].

fragmentation function the behaviour

$$D_{\mathrm{NP}}(x) \propto f\left((1-x)\frac{m}{\Lambda}\right), \tag{8.3}$$

where f is a function that vanishes when its argument becomes much larger than one, Λ is a hadronic scale, and m is the mass of the heavy quark. This yields, in moment space, the behaviour

$$D_{\mathrm{NP}}(N) = 1 - (N-1)\,\Lambda/m \int f(z)\,z\,dz + \mathcal{O}(\Lambda^2/m^2)\,. \tag{8.4}$$

If $D_{\mathrm{NP}}(N)$ depends upon a single parameter, its value can be linked to the ratio Λ/m. For example, in the case of the form (8.2) the series expansion in powers of $1/\alpha$ is given by

$$D_{\mathrm{NP}}(N) = 1 - (N-1)\frac{2}{\alpha} + \mathcal{O}\left(\frac{1}{\alpha^2}\right)\,. \tag{8.5}$$

Reinterpreting $\alpha \to 2\,m/\Lambda$ we will be able to check the behaviour of the leading power correction. Using $\Lambda \sim 300$ MeV, $m_c \simeq 1.5$ GeV and $m_b \simeq 4.75$ GeV, one expects to find $\alpha_D \sim 10$ and $\alpha_B \sim 30$ when fitting D/D^* and B mesons respectively. Whatever the exact values are, it will always be possible to test for the predicted scaling law

$$\frac{\alpha_B}{\alpha_D} \simeq \frac{m_b}{m_c} \sim 3\,. \tag{8.6}$$

To this end, we extract the value of α for B meson production at Z^0 energy. In figure 21 we show the fits to the four available data sets. All the data appear consistent with each other. Within fairly large uncertainties (resulting from the non-constancy of α
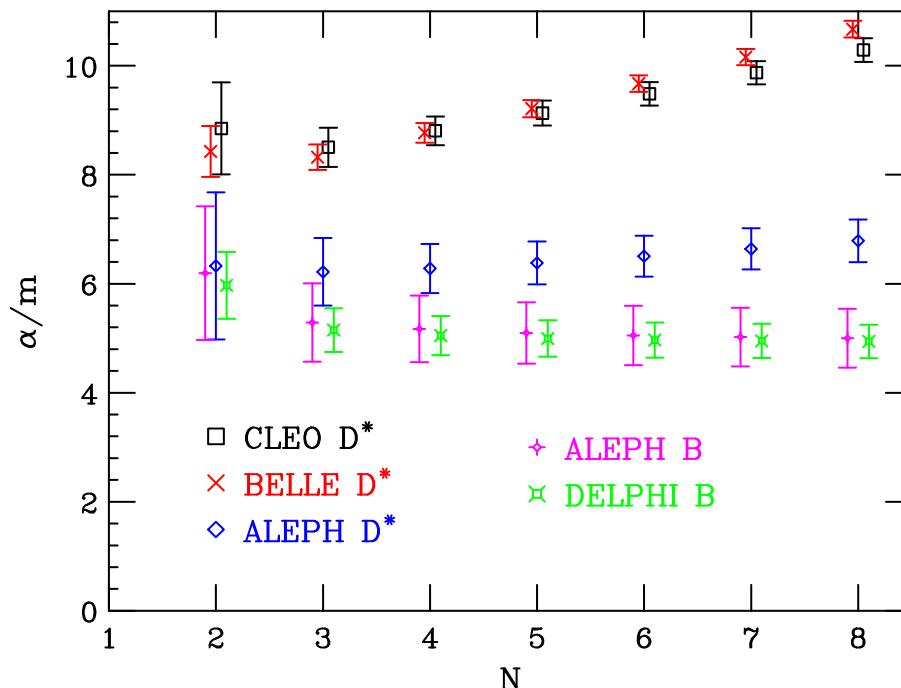
Figure 22: Values of α/m for D^* and B mesons as a function of N.

through the fits to different moments, and the discrepancy between the determination of α_D at M_Υ and M_Z) we can see that the expectations are largely fulfilled, leading to an α_B/α_D ratio of order 1.5 to 3. The tendency for values smaller than $m_b/m_c = 3.17$ might be a consequence of a number of factors, like the B data being for "weakly decaying" B's, and therefore generally softer than the leading B^* and B^{**}, or the mass entering the power corrections being closer to the meson mass rather than the quark mass.

It is also worth noting that, given a value for $\alpha_B \simeq 25$, the expectations for the value of the ratio are much better fulfilled if we use the α_D fitted at the Z energy ($\alpha_D \simeq 9$) rather than the one fitted at the $\Upsilon(4S)$ energy ($\alpha_D \simeq 14$), as shown in figure 22. This result mildly supports the view that large non-perturbative corrections may affect the $\Upsilon(4S)$ data.

The results of figures 19 and 20 are also summarized in table 4, together with similar results for the one-parameter forms of ref. [44] and with the popular PSSZ form [43].[12] Results for B mesons are also shown in table 4.

---

[12]The values of ϵ that we find in this case are about one order of magnitude smaller than those usually extracted from Monte Carlo simulations. They lead, therefore, to a harder non-perturbative fragmentation function and hence to larger rates in hadronic collisions. It is moreover worth noting that the use of the PSSZ fragmentation function in a context where non-perturbative corrections are expected to scale like $1 - (N-1)\Lambda/m$ is inconsistent. In fact, while the ϵ parameter can be interpreted as being of order Λ^2/m^2 [43], the series expansion of its Mellin transform can be shown to be

$$D_{\mathrm{NP}}(N) = 1 + \frac{2(\log \epsilon - 1)(N-1) + 4N(\psi^{(0)}(N) + \gamma_E)}{\pi}\sqrt{\epsilon} + \mathcal{O}(\epsilon).\tag{8.7}$$

The presence of the $\log \epsilon$ term in the coefficient of the term linear in $\sqrt{\epsilon}$ does not allow to interpret it as a simple Λ/m power correction.

N	2	3	4	5	6	7	8
$\sigma_Q(N,q^2,m^2) = \langle x^{N-1}\rangle_{\mathrm{pQCD}}$							
c @ 10.58 GeV	0.7359	0.5749	0.4601	0.3778	0.3167	0.2698	0.2331
c @ 91.2 GeV (NS)	0.5858	0.3937	0.2843	0.2151	0.1683	0.1345	0.1107
c @ 91.2 GeV (full)	0.5954	0.3988	0.2860	0.2158	0.1686	0.1353	0.1108
b @ 91.2 GeV	0.7634	0.6280	0.5309	0.4590	0.4033	0.3587	0.3222
Experimental data (norm. to one)							
BELLE $D^{*+} \to D^0$ (ISR corr.)	0.6418 ± 0.0042	0.4399 ± 0.0028	0.3169 ± 0.0020	0.2375 ± 0.0015	0.1838 ± 0.0012	0.1462 ± 0.0010	0.1189 ± 0.0009
ALEPH D^{*+} (ISR corr.)	0.4920 ± 0.0152	0.2803 ± 0.0075	0.1748 ± 0.0047	0.1160 ± 0.0033	0.0806 ± 0.0025	0.0582 ± 0.0020	0.0432 ± 0.0016
ALEPH B	0.7163 ± 0.0085	0.5433 ± 0.0097	0.4269 ± 0.0098	0.3437 ± 0.0096	0.2819 ± 0.0094	0.2345 ± 0.0091	0.1975 ± 0.0087
$D_{\mathrm{NP}}(N) = \langle x^{N-1}\rangle_{\mathrm{NP}}$							
CLEO D^{*+}	$0.877^{+0.009}_{-0.010}$	$0.769^{+0.007}_{-0.007}$	$0.690^{+0.006}_{-0.006}$	$0.626^{+0.006}_{-0.006}$	$0.576^{+0.006}_{-0.006}$	$0.534^{+0.006}_{-0.006}$	$0.500^{+0.006}_{-0.006}$
BELLE $D^{*+} \to D^0$	$0.872^{+0.005}_{-0.006}$	$0.765^{+0.005}_{-0.005}$	$0.689^{+0.004}_{-0.004}$	$0.629^{+0.004}_{-0.004}$	$0.580^{+0.004}_{-0.004}$	$0.542^{+0.004}_{-0.004}$	$0.510^{+0.004}_{-0.004}$
ALEPH D^{*+}	$0.840^{+0.022}_{-0.031}$	$0.712^{+0.018}_{-0.021}$	$0.615^{+0.016}_{-0.017}$	$0.539^{+0.015}_{-0.016}$	$0.479^{+0.014}_{-0.015}$	$0.430^{+0.014}_{-0.015}$	$0.391^{+0.014}_{-0.015}$
Tab. 2 and eq. (4.2)	0.868	0.767	0.688	0.626	0.576	0.536	0.503
ALEPH B	$0.938^{+0.009}_{-0.014}$	$0.865^{+0.014}_{-0.018}$	$0.804^{+0.017}_{-0.020}$	$0.749^{+0.019}_{-0.023}$	$0.699^{+0.022}_{-0.025}$	$0.654^{+0.024}_{-0.027}$	$0.613^{+0.025}_{-0.029}$
SLD B	$0.931^{+0.016}_{-0.030}$	$0.850^{+0.019}_{-0.025}$	$0.781^{+0.020}_{-0.024}$	$0.718^{+0.021}_{-0.024}$	$0.661^{+0.021}_{-0.024}$	$0.610^{+0.021}_{-0.024}$	$0.563^{+0.022}_{-0.024}$
KLP α							
CLEO D^{*+}	13.28 ± 1.27	12.76 ± 0.54	13.21 ± 0.40	13.70 ± 0.34	14.23 ± 0.32	14.81 ± 0.32	15.43 ± 0.33
BELLE $D^{*+} \to D^0$	12.64 ± 0.70	12.49 ± 0.35	13.16 ± 0.27	13.82 ± 0.24	14.51 ± 0.23	15.24 ± 0.23	16.01 ± 0.23
ALEPH D^{*+}	9.49 ± 2.03	9.33 ± 0.93	9.42 ± 0.68	9.58 ± 0.59	9.76 ± 0.56	9.96 ± 0.57	10.18 ± 0.59
ALEPH B	29.42 ± 5.82	25.12 ± 3.41	24.56 ± 2.90	24.22 ± 2.67	24.00 ± 2.58	23.86 ± 2.56	23.75 ± 2.57
ALEPH B, $m_b = 4.5$ GeV	34.32 ± 7.77	28.26 ± 4.23	27.34 ± 3.51	26.73 ± 3.18	26.34 ± 3.04	26.07 ± 2.98	25.87 ± 2.97
ALEPH B, $m_b = 5.0$ GeV	25.90 ± 4.59	22.72 ± 2.84	22.41 ± 2.46	22.23 ± 2.30	22.13 ± 2.25	22.07 ± 2.24	22.03 ± 2.26
SLD B	25.87 ± 8.66	22.11 ± 3.80	21.33 ± 2.75	20.73 ± 2.25	20.27 ± 1.98	19.89 ± 1.82	19.57 ± 1.72
BCFY r							
CLEO D^{*+}	0.0531 ± 0.0077	0.0610 ± 0.0036	0.0615 ± 0.0026	0.0611 ± 0.0021	0.0601 ± 0.0019	0.0587 ± 0.0017	0.0569 ± 0.0016
BELLE $D^{*+} \to D^0$	0.0570 ± 0.0046	0.0628 ± 0.0025	0.0618 ± 0.0018	0.0604 ± 0.0014	0.0585 ± 0.0013	0.0564 ± 0.0011	0.0541 ± 0.0011
ALEPH D^{*+}	0.0849 ± 0.0247	0.0936 ± 0.0125	0.0972 ± 0.0092	0.0988 ± 0.0080	0.0993 ± 0.0074	0.0990 ± 0.0072	0.0981 ± 0.0072
ALEPH D^{*+}, $m_c = 1.3$ GeV	0.0470 ± 0.0238	0.0557 ± 0.0102	0.0594 ± 0.0074	0.0613 ± 0.0063	0.0621 ± 0.0059	0.0623 ± 0.0057	0.0619 ± 0.0057
ALEPH D^{*+}, $m_c = 1.7$ GeV	0.1198 ± 0.0289	0.1288 ± 0.0146	0.1323 ± 0.0108	0.1336 ± 0.0093	0.1337 ± 0.0086	0.1329 ± 0.0084	0.1315 ± 0.0084
PSSZ ϵ ($\times 10^2$)							
BELLE $D^{*+} \to D^0$	0.234 ± 0.032	0.271 ± 0.019	0.260 ± 0.013	0.246 ± 0.010	0.230 ± 0.009	0.213 ± 0.007	0.197 ± 0.007
ALEPH D^{*+}	0.473 ± 0.245	0.548 ± 0.129	0.574 ± 0.096	0.580 ± 0.081	0.575 ± 0.074	0.563 ± 0.071	0.547 ± 0.069
ALEPH B	0.028 ± 0.014	0.047 ± 0.016	0.056 ± 0.016	0.062 ± 0.017	0.068 ± 0.018	0.073 ± 0.019	0.077 ± 0.020

Table 4: Summary of results for the first eight moments. The first group of lines (labelled $\sigma_Q(N,q^2,m^2) = \langle x^{N-1}\rangle_{\mathrm{pQCD}}$) gives perturbative moments for c and b production at the $\Upsilon(4S)$ and Z^0 energies. The second group (labelled "Experimental data") gives the measured moments when explicitly given by the experimental Collaborations. In this case, the ISR correction (when applied) has been taken from the right panel of figure 3. The third group (labelled $D_{\mathrm{NP}}(N) = \langle x^{N-1}\rangle_{\mathrm{NP}}$) gives the moments of the non-perturbative fragmentation function that we extracted from the data. The last three groups report the value of the parameters of the KLP, BCFY and PSSZ parametrization extracted from several data sets.
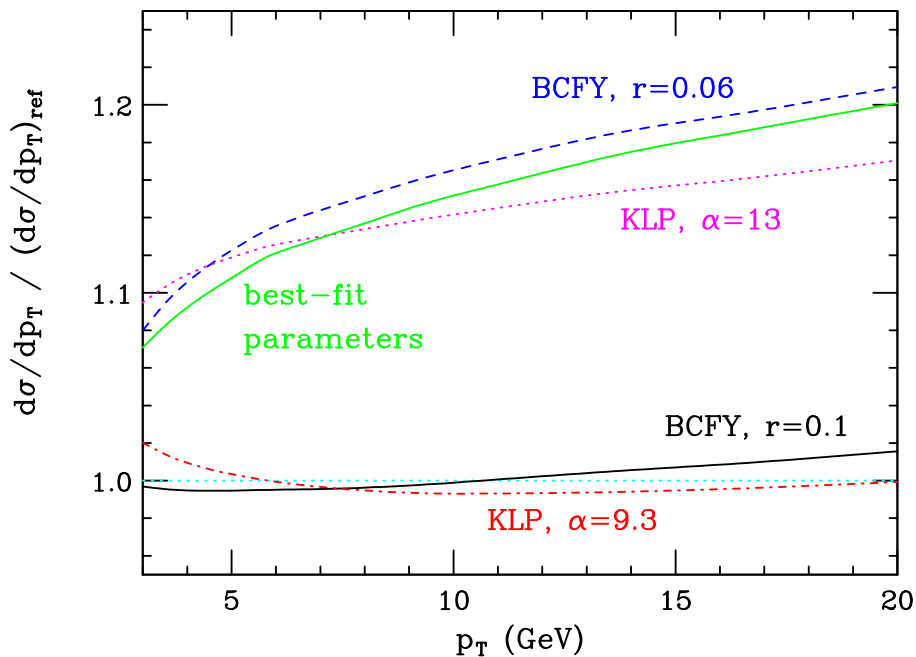
Figure 23: Ratios between new evaluations of the $d\sigma/dp_T$ production cross section of D^* mesons in $p\bar{p}$ collisions at the Tevatron Run II and the value originally published in [32], $(d\sigma/dp_T)_{\rm ref}$.

8.2 Implications for heavy-flavour hadroproduction

It is legitimate to ask what is the impact of the new, high precision $\Upsilon(4S)$ data on the calculation of D meson production spectra in hadronic collisions, especially in view of the discrepancy between $\Upsilon(4S)$ and Z^0 data. The question has not, however, a straightforward answer. If the discrepancy is related to a power suppressed effect in the e^+e^- coefficient functions, one should then privilege the Z^0 data, where power effects are much reduced. It is worth noting, however, that if we instead use the $\Upsilon(4S)$ data, the impact on the hadronic cross sections is quite limited. This is clearly visible in figure 19, where it appears that for N around 5 the $\Upsilon(4S)$ moments are higher than the Z^0 ones by roughly 20%. This value is directly proportional to the D^* production cross section in hadron collisions at large p_T. Therefore, in this 'worst case' scenario, having used the ALEPH data (the only accurate ones available at the time), might have lead ref. [32] to underestimate the D^* hadronic cross section by 20%, an uncertainty which is anyway not larger than those of purely perturbative origin (variation of renormalization and factorization scales) or stemming from the parton distribution functions.

These considerations are put on a more quantitative footing in figure 23, where we plot the ratios between new determinations of the p_T distribution of D^* production at the Tevatron Run II and the central value obtained in ref. [32]. The solid line, labeled 'BCFY, r = 0.1' is obtained by employing the same non-perturbative fragmentation function and the same parameter $r = 0.1$ as in [32]. Its small difference from one is essentially of perturbative origin. It is due to the different treatment of the perturbative fragmentation function in the FONLL code for heavy quark hadronic production [45, 46] which, for consistency
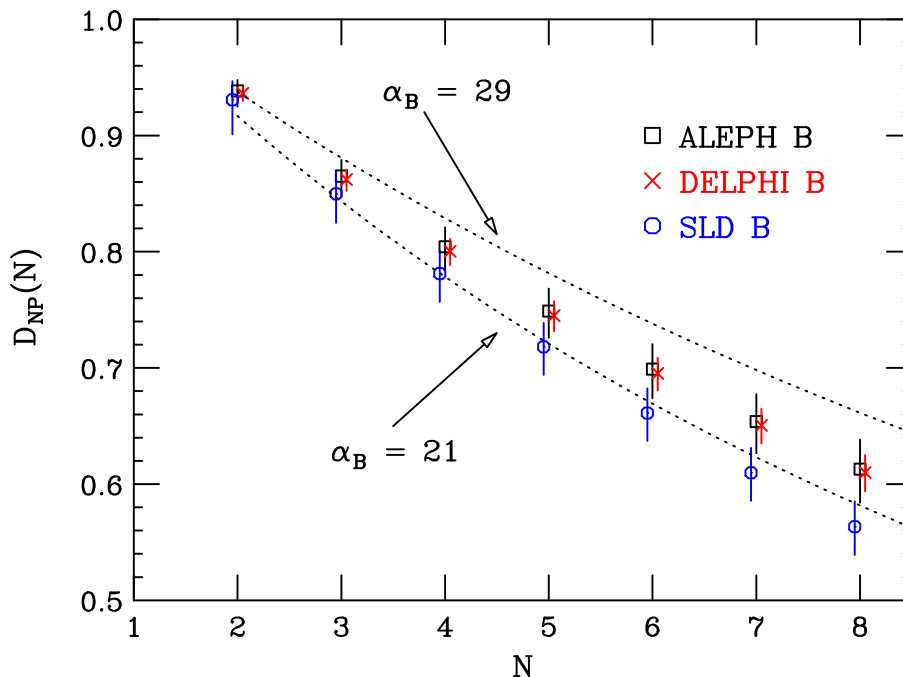
Figure 24: Non-perturbative moments from weakly decaying B's data.

with the extraction of the non-perturbative parameters, has been modified to include also the Sudakov resummation for the initial condition and the large-N regularization procedure described in eq. (2.45). The five other curves are instead obtained with different non-perturbative forms and/or parameters relative to the $\Upsilon(4S)$ or to the Z^0 results from table 4. As expected, using a different functional form (KLP) but a parameter also extracted from the ALEPH data ($\alpha = 9.3$) returns a result very similar to that of ref. [32]. On the other hand, using determinations from CLEO/BELLE data ($\alpha = 13$) returns a larger cross section, the increase being of the order predicted above and not larger than the uncertainties of perturbative origin.

As far as B mesons are concerned, the values for α_B are translated into non-perturbative moments in figure 24. The dotted band shows the values given by two extreme choices of α_B. One can see that, using everywhere the value determined at $N = 2$, i.e. $\alpha_B \simeq 29$, as done in [39],[13] only overestimates the moment at $N = 4$ by a few percent. Up to $N = 8$ the difference is never larger than 10%. Such an uncertainty is fully acceptable when calculating the hadronic production of B mesons, given the similar or larger size of the perturbative uncertainties and of those due to the parton distribution functions.

9. Conclusions

In the present paper, we have obtained two main results. First, we have shown that it is

---

[13]In this reference, a pure NLL collinear resummation was used, without Sudakov resummation and large-N correction factor. This does not affect, of course, the small-N region, hence the determination of a very similar value for α_B.

possible to perform excellent fits of D and B meson fragmentation spectra in perturbative QCD, using all known results on the perturbative heavy-quark fragmentation function, and compounding them with a simple parametrization of non-perturbative effects. For reasons of space we did not perform fits to available data on D_s and Λ_c production. We can provide the corresponding results upon request.

A second striking result is the evidence of large non-perturbative effects, visible in the relation between the D^* fragmentation function at the $\Upsilon(4S)$ and Z^0 energies. It would be interesting to understand the power law of these contributions. Their magnitude would suggest a $1/E$ scaling law. Theoretical arguments based upon infrared renormalons would favour, instead, a $1/E^2$ behaviour. Because of the lack of precise D production data in the intermediate region, it is difficult, at this point, to discriminate between the two possibilities. We point out, however, that, if these non-perturbative corrections involve the coefficient functions, they may be present also in light-hadron production, where data at intermediate energy are available. It is thus possible that fits to the light-hadron fragmentation functions from $\Upsilon(4S)$ up to Z^0 energies may clarify this issue.

The parametrization of the non-perturbative component of the heavy-quark fragmentation function is also relevant for the calculation of heavy-quark hadroproduction cross sections. In the present work we provide various related results, that can be used for such calculations.

Acknowledgments

References

[1] B. Mele and P. Nason, *The fragmentation function for heavy quarks in QCD*, *Nucl. Phys.* **B 361** (1991) 626.

[2] M. Cacciari and S. Catani, *Soft-gluon resummation for the fragmentation of light and heavy quarks at large x*, *Nucl. Phys.* **B 617** (2001) 253 [hep-ph/0107138].

[3] CLEO collaboration, M. Artuso et al., *Charm meson spectra in e^+e^- annihilation at 10.5 GeV c.m.e.*, *Phys. Rev.* **D 70** (2004) 112001 [hep-ex/0402040].

[4] BELLE collaboration, R. Seuster et al., *Charm hadrons from fragmentation and B decays in e^+e^- annihilation at $\sqrt{s} = 10.6$ GeV*, *Phys. Rev.* **D 73** (2006) 032002 [hep-ex/0506068].

[5] ALEPH collaboration, A. Heister et al., *Study of the fragmentation of b quarks into B mesons at the Z peak*, *Phys. Lett.* **B 512** (2001) 30 [hep-ex/0106051].

[6] OPAL collaboration, G. Abbiendi et al., *Inclusive analysis of the b quark fragmentation function in Z decays at LEP*, *Eur. Phys. J.* **C 29** (2003) 463 [hep-ex/0210031].

[7] SLD collaboration, K. Abe et al., *Measurement of the b-quark fragmentation function in Z^0 decays*, *Phys. Rev.* **D 65** (2002) 092006 [hep-ex/0202031].

[8] DELPHI collaboration, G. Baker et. al., *A study of the b-quark fragmentation function with the DELPHI detector at LEP I*, DELPHI 2002-069 CONF 603, http://delphiwww.cern.ch/pubxx/delnote/public/2002%5F069%5Fconf%5F603.ps.gz.

[9] E. Ben-haim, *The b quark fragmentation function, from LEP to Tevatron*, FERMILAB-THESIS-2004-50.

[10] M. Cacciari, P. Nason and C. Oleari, *Crossing heavy-flavour thresholds in fragmentation functions*, *JHEP* **10** (2005) 034 [hep-ph/0504192].

[11] ALEPH collaboration, R. Barate et al., *Study of charm production in Z decays*, *Eur. Phys. J.* **C 16** (2000) 597 [hep-ex/9909032].

[12] P. Nason and B.R. Webber, *Scaling violation in e^+e^- fragmentation functions: QCD evolution, hadronization and heavy quark mass effects*, *Nucl. Phys.* **B 421** (1994) 473, [erratum *ibid.* **480** (1996) 755].

[13] G. Altarelli and G. Parisi, *Asymptotic freedom in parton language*, *Nucl. Phys.* **B 126** (1977) 298.

[14] G. Curci, W. Furmanski and R. Petronzio, *Evolution of parton densities beyond leading order: the nonsinglet case*, *Nucl. Phys.* **B 175** (1980) 27.

[15] W. Furmanski and R. Petronzio, *Singlet parton densities beyond leading order*, *Phys. Lett.* **B 97** (1980) 437.

[16] E.G. Floratos, C. Kounnas and R. Lacaze, *Higher order QCD effects in inclusive annihilation and deep inelastic scattering*, *Nucl. Phys.* **B 192** (1981) 417.

[17] J. Kalinowski, K. Konishi, P.N. Scharbach and T.R. Taylor, *Resolving QCD jets beyond leading order: quark decay probabilities*, *Nucl. Phys.* **B 181** (1981) 253.

[18] J. Kalinowski, K. Konishi and T.R. Taylor, *Jet calculus beyond leading logarithms*, *Nucl. Phys.* **B 181** (1981) 221.

[19] K. Melnikov and A. Mitov, *Perturbative heavy quark fragmentation function through $O(\alpha_s^2)$*, *Phys. Rev.* **D 70** (2004) 034027 [hep-ph/0404143].

[20] A. Mitov, *Perturbative heavy quark fragmentation function through $O(\alpha_s^2)$: gluon initiated contribution*, *Phys. Rev.* **D 71** (2005) 054021 [hep-ph/0410205].

[21] M. Cacciari and E. Gardi, *Heavy-quark fragmentation*, *Nucl. Phys.* **B 664** (2003) 299 [hep-ph/0301047].

[22] A.V. Manohar, *Deep inelastic scattering as $x \to 1$ using soft-collinear effective theory*, *Phys. Rev.* **D 68** (2003) 114019 [hep-ph/0309176].

[23] P. Nason and B.R. Webber, *Non-perturbative corrections to heavy quark fragmentation in e^+e^- annihilation*, *Phys. Lett.* **B 395** (1997) 355 [hep-ph/9612353].

[24] R.L. Jaffe and L. Randall, *Heavy quark fragmentation into heavy mesons*, *Nucl. Phys.* **B 412** (1994) 79 [hep-ph/9306201].

[25] L. Randall and N. Rius, *Using heavy quark fragmentation into heavy hadrons to determine QCD parameters and test heavy quark symmetry*, *Nucl. Phys.* **B 441** (1995) 167 [hep-ph/9405217].

[26] M. Dasgupta and B.R. Webber, *Power corrections and renormalons in fragmentation functions*, *Nucl. Phys.* **B 484** (1997) 247 [hep-ph/9608394].

[27] E.A. Kuraev and V.S. Fadin, *On radiative corrections to e^+e^- single photon annihilation at high-energy*, *Sov. J. Nucl. Phys.* **41** (1985) 466.

[28] G. Altarelli and G. Martinelli, *Radiative corrections to the Z^0 line shape at LEP*, in J. Ellis, R.D. Peccei, eds., Physics At Lep, Vol. 1*, 47-57.

[29] O. Nicrosini and L. Trentadue, *Soft photons and second order radiative corrections to $e^+e^- \to Z^0$*, *Phys. Lett.* **B 196** (1987) 551.

[30] O. Nicrosini and L. Trentadue, *Second order electromagnetic radiative corrections to $e^+e^- \to \gamma^*$, $Z^0 \to \mu^+\mu^-$*, *Z. Physik* **C 39** (1988) 479.

[31] G. Colangelo and P. Nason, *A theoretical study of the c and b fragmentation function from e^+e^- annihilation*, *Phys. Lett.* **B 285** (1992) 167.

[32] M. Cacciari and P. Nason, *Charm cross sections for the Tevatron Run II*, *JHEP* **09** (2003) 006 [hep-ph/0306212].

[33] PARTICLE DATA GROUP collaboration, S. Eidelman et al., *Review of particle physics*, *Phys. Lett.* **B 592** (2004) 1.

[34] CLEO collaboration, R. Ammar et al., *Measurement of the total cross section for $e^+e^- \to$ hadrons at $\sqrt{s} = 10.52$ GeV*, *Phys. Rev.* **D 57** (1998) 1350 [hep-ex/9707018].

[35] M. Beneke, V.M. Braun and L. Magnea, *Phenomenology of power corrections in fragmentation processes in e^+e^- annihilation*, *Nucl. Phys.* **B 497** (1997) 297 [hep-ph/9701309].

[36] P. Nason and C. Oleari, *A phenomenological study of heavy-quark fragmentation functions in e^+e^- annihilation*, *Nucl. Phys.* **B 565** (2000) 245 [hep-ph/9903541].

[37] S. Frixione, M.L. Mangano, P. Nason and G. Ridolfi, *Heavy-quark production*, *Adv. Ser. Direct. High Energy Phys.* **15** (1998) 609–706 [hep-ph/9702287].

[38] P. Nason et al., *Bottom production*, in the *1999 CERN Workshop on Standard Model Physics (and more) at the LHC*, CERN, Geneva, Switzerland, 25–26 May 1999 - CERN, Geneva, 2000, (CERN-2000-004) - pp. 231, 1999, hep-ph/0003142.

[39] M. Cacciari and P. Nason, *Is there a significant excess in bottom hadroproduction at the Tevatron?*, *Phys. Rev. Lett.* **89** (2002) 122003 [hep-ph/0204025].

[40] M. Cacciari, S. Frixione, M.L. Mangano, P. Nason and G. Ridolfi, *QCD analysis of first b cross section data at 1.96 TeV*, *JHEP* **07** (2004) 033 [hep-ph/0312132].

[41] M. Cacciari, P. Nason and R. Vogt, *QCD predictions for charm and bottom production at RHIC*, *Phys. Rev. Lett.* **95** (2005) 122001 [hep-ph/0502203].

[42] V.G. Kartvelishvili, A.K. Likhoded and V.A. Petrov, *On the fragmentation functions of heavy quarks into hadrons*, *Phys. Lett.* **B 78** (1978) 615.

[43] C. Peterson, D. Schlatter, I. Schmitt and P.M. Zerwas, *Scaling violations in inclusive e^+e^- annihilation spectra*, *Phys. Rev.* **D 27** (1983) 105.

[44] E. Braaten, K.-m. Cheung, S. Fleming and T.C. Yuan, *Perturbative QCD fragmentation functions as a model for heavy quark fragmentation*, *Phys. Rev.* **D 51** (1995) 4819 [hep-ph/9409316].

[45] M. Cacciari, M. Greco and P. Nason, *The p_T spectrum in heavy-flavour hadroproduction*, *JHEP* **05** (1998) 007 [hep-ph/9803400].

[46] M. Cacciari, S. Frixione and P. Nason, *The p_T spectrum in heavy-flavor photoproduction*, *JHEP* **03** (2001) 006 [hep-ph/0102134].